Accepted Manuscript

Free fatty acid receptor 1 (GPR40) agonists containing spirocyclic periphery inspired by LY2881835

Mikhail Krasavin, Alexey Lukin, Daria Bagnyukova, Nikolay Zhurilo, Ihor Zahanich, Sergey Zozulya, Jouni Ihalainen, Markus M. Forsberg, Marko Lehtonen, Jarkko Rautio, Daniel Moore, Irina G. Tikhonova
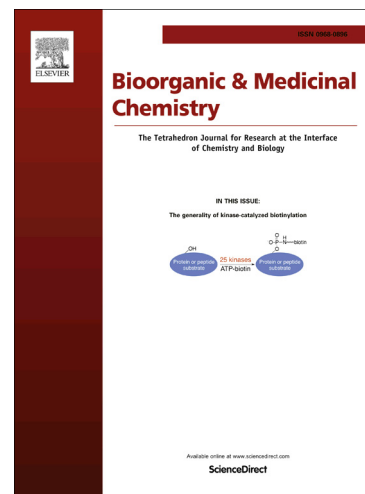
Please cite this article as: Krasavin, M., Lukin, A., Bagnyukova, D., Zhurilo, N., Zahanich, I., Zozulya, S., Ihalainen, J., Forsberg, M.M., Lehtonen, M., Rautio, J., Moore, D., Tikhonova, I.G., Free fatty acid receptor 1 (GPR40) agonists containing spirocyclic periphery inspired by LY2881835, *Bioorganic & Medicinal Chemistry* (2016), doi: http://dx.doi.org/10.1016/j.bmc.2016.09.004

Free fatty acid receptor 1 (GPR40) agonists containing spirocyclic periphery inspired by LY2881835

Mikhail Krasavin,[*] Alexey Lukin, Daria Bagnyukova, Nikolay Zhurilo, Ihor Zahanich, Sergey Zozulya, Jouni Ihalainen, Markus M. Forsberg, Marko Lehtonen, Jarkko Rautio, Daniel Moore, and Irina G. Tikhonova
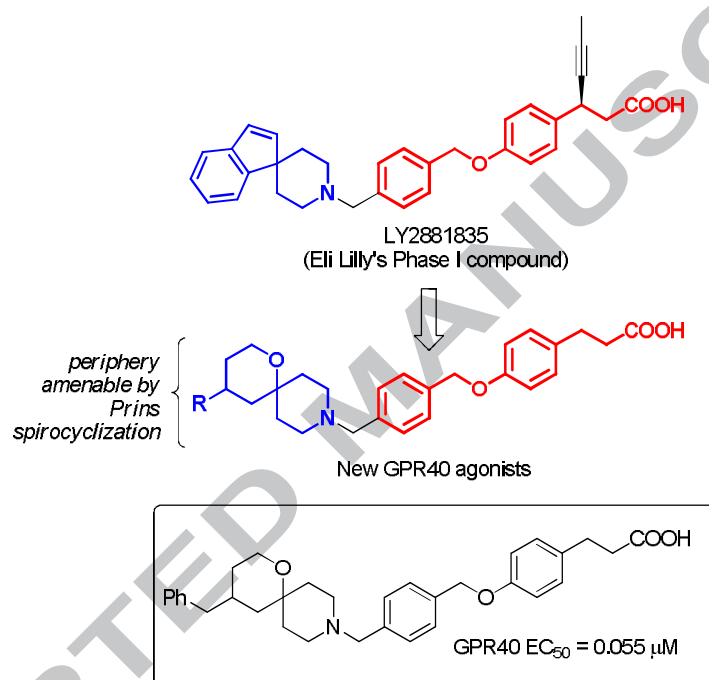
Free fatty acid receptor 1 (GPR40) agonists containing spirocyclic periphery inspired by LY2881835

Mikhail Krasavin,[a, *] Alexey Lukin,[b] Daria Bagnyukova,[b] Nikolay Zhurilo,[b] Ihor Zahanich,[c] Sergey Zozulya, [c, d] Jouni Ihalainen,[e] Markus M. Forsberg,[e] Marko Lehtonen,[e] Jarkko Rautio,[e] Daniel Moore,[f] and Irina G. Tikhonova[f]

[a] *Saint Petersburg State University, Saint Petersburg, 199034 Russian Federation*

[b] *Lomonosov Institute of Fine Chemical Technologies, Moscow Technological University, 86 Vernadskogo Prospekt, Moscow, 117571 Russian Federation*

[c] *Enamine Ltd, 78 Chervonotkatska, Kyiv 02094, Ukraine*

[d] *Taras Shevchenko National University, 62 Volodymyrska, Kyiv 01033, Ukraine*

[e] *School of Pharmacy, University of Eastern Finland, 70211 Kuopio, Finland*

[f] *Molecular Therapeutics, School of Pharmacy, Medical Biology Centre, Queen's University Belfast, Belfast BT9 7BL, Northern Ireland, UK*

* Corresponding author; phone: + 7 931 3617872, fax: +7 812 428 6939.
E-mail address: m.krasavin@spbu.ru

ABSTRACT

The free fatty acid receptor 1 (FFA1), a G protein-coupled receptor (GPCR) naturally activated by long-chain fatty acids is a novel target for the treatment of metabolic diseases. The basic amine spirocyclic periphery of Eli Lilly's drug candidate LY2881835 for treatment of type 2 diabetes mellitus (which reached phase I clinical trials) inspired a series of novel FFA1 agonists. These were designed to incorporate the 3-[4-(benzyloxy)phenyl]propanoic acid pharmacophore core decorated with a range of spirocyclic motifs. The latter were prepared via the Prins cyclization and subsequent modification of the 4-hydroxytetrahydropyran moiety in the Prins product. Here, we synthesize 19 compounds and test for FFA1 activity. Within this pilot set, a nanomolar potency ($EC_{50} = 55$ nM) was reached. Four lead compounds (EC_{50} range 55 – 410 nM) were characterized for aqueous solubility, metabolic stability, plasma protein binding and Caco-2 permeability. While some instability in the presence of mouse liver microsomes was noted, mouse pharmacokinetic profile of the compound having the best overall ADME properties was evaluated to reveal acceptable bioavailability (F = 10.3%) and plasma levels achieved on oral administration.

Keywords:

GPCR, GPR40, free fatty acid receptor 1, FFA1 agonists, type 2 diabetes mellitus, Prins reaction, spirocyclic motifs, metabolic stability.

1. Introduction

The free fatty acid receptor 1 (FFA1, known as GPR40 prior to its de-orphaning in 2003) promptly became a biological target of high importance from the standpoint of developing fundamentally new therapeutic agents against type 2 diabetes mellitus (T2DM). FFA1 agonists are capable of raising insulin levels but only do so in hyperglycemic state when the FFA1 expression is upregulated.[1] The activation of FFA1 triggers a GPCR signaling cascade which invokes insulin secretion to normalize blood glucose levels. As a result, the expression of the receptor goes back to normal, desensitizing the insulin-producing machinery to FFA1 agonists still remaining in circulation.[2] This is in sharp contrast to other antidiabetic agents, such as sulfonylureas, that continue stimulating insulin release irrespective of the current glucose levels and can, therefore, cause hypoglycemia (an adverse, potentially deadly condition).

The extensive worldwide research efforts in the decade following FFA1 de-orphaning aimed at developing clinically useful FFA1 agonists[3] were nearly halted after Takeda's first-in-class agent fasiglifam (TAK-875) was discontinued in phase III of human trials.[4] On the date of submission of this manuscript, only one FFA1 agonist (Piramal's compound P11187 of undisclosed structure) was in clinical research.[5] This is rather unfortunate since the efficacy profile of TAK-875 established in its clinical trials was very good (despite the observed idiosyncratic liver toxicity that led to the discontinuation).[6] Therefore, if the toxicity profile of FFA1 agonists is diligently tackled, there remains an opportunity to bring the first drug in this class to market.[7]

The toxicity of TAK-875 was debatably linked to its overly high lipophilicity.[7] On the one hand, relatively high lipophilicity is likely a pre-requisite for ligand's affinity to the receptor (considering the fact that its endogenous ligands are medium-to-long chain fatty acids[1]). On the other hand increasing the polarity (i. e. increasing the total polar surface area or lowering the LogP) of FFA1 agonists could provide the solution to the toxicity problem. Recently, we reported potent and selective FFA1 agonists based on containing 1,3-oxazole, 1,2,4-oxadiazole[8] and 1,2,4-thiadiazole[9-10] grafted onto or replacing the phenyl ring of the 3-[4-(benzyloxy)phenyl]propanoic acid core, which mimics the fatty acid endogenous ligands of the receptor and is present in TAK-875 and other advanced compounds of this class (such as Amgen's AMG-837,[3] and Eli Lilly's LY2881835[3]) (Figure 1).

Figure 1. Advanced GPR40 agonists containing the 3-[4-(benzyloxy)phenyl]propanoic acid core.
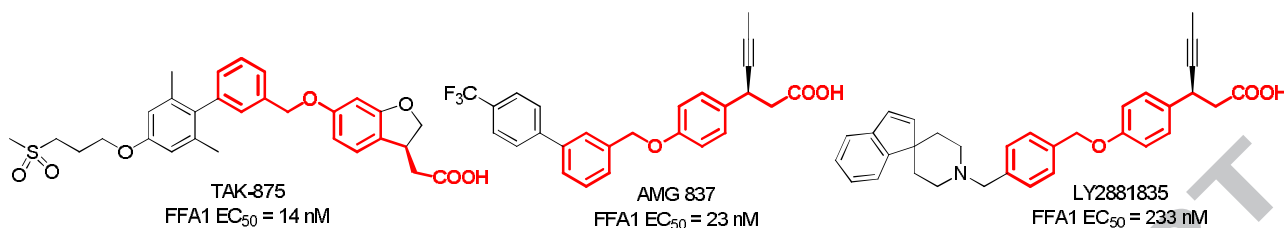

Besides the heterocyclic appendage[8] or scaffold hopping[9-10] approach realized in our previous studies, we became intrigued by the structure of LY2881835 and the presence of a basic amine center, in combination with the spirocyclic motif, in its periphery. Both aspects appeared quite appealing from the drug design standpoint. The basic center, which would likely be protonated at physiological pH, is capable of increasing hydrophilic character of LY2881835 itself or any related compounds. This was clearly a reassuring observation as high lipophilicity has been dogmatized as a pre-requisite to high ligand affinity toward FFA1 (we observed a significant activity drop on replacing the 3-phenylpropionic acid FFA1 pharmacophore with its more polar 1,3,4-thiadiazole congener[9]). Spirocyclic moieties are considered privileged moieties in GPCR ligand design due to their pronounced three-dimensional character, which ensures better complementarity of a small-molecule ligand to its protein target and, as a result, fewer off-target effects.[11]

The Prins cyclization involving cyclic ketones and homoallylic alcohol under Lewis or Brønsted acid catalysis provides a facile entry into spirocyclic motifs which contain a potentially reactive functionality originating from the interception of intermediate spirocyclic carbocation with various nucleophiles (thus resulting in a formal three-component process).[12] Azacycloalkanones have been rarely employed as carbonyl components in the Prins cyclization, except for a comprehensive methodology report from the Ghosh group.[13] Recently, we described a facile and convenient protocol to prepare spirocyclic amino alcohol building blocks from a range of azacycloalkanones.[14] In particular, *N*-Boc-protected 1-oxa-9-azaspiro[5.5]undecan-4-ol (**1**) which was amenable by this method on a multigram scale, was viewed as a particularly valuable building block to graft diverse spirocyclic periphery, similar to that of LY2881835, onto the 3-[4-(benzyloxy)phenyl]propanoic acid core, which common to many advanced FFA1 agonists (*vide supra*), via a reductive amination of aldehyde building block **2** with a range of amines **3** derived from **1**.

While **2** was lacking a substituent in position 3 of 3-phenylpropanoic carboxylate (which is present in many advanced compounds shown in Figure 1), we reasoned that the use of the simplified pharmacophore would allow streamlined screening for the optimal spirocyclic periphery in series **4**. Once lead compounds are identified within the latter, appropriate substitutions in the 3-[4-(benzyloxy)phenyl]propanoic acid portion of the future new agonists can be defined and introduced

(Figure 2). Herein, we describe the initial promising results related to the synthesis, biological and ADMET/PK profiling of compounds belonging to series **4**.

Figure 2. Design and retrosynthetic analysis of new series of FFA1 agonists **4**.
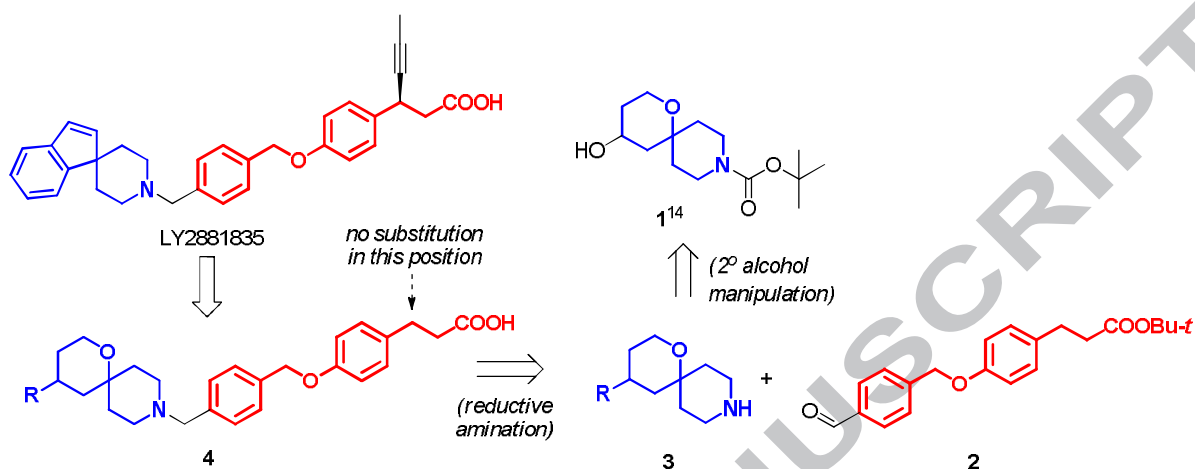
2. Results and discussion

The synthesis of core aldehyde building block **2** commenced with known[15] aldehyde **5**. The Horner-Wadsworth-Emmons olefination of the latter (using commercially available **6**) gave cinnamate ester **7**. Facile hydrogenation of the double bond in **7** was achieved over Raney nickel without the disruption of the benzyl ether. Selective hydrolysis of the methyl ester in resulting *tert*-butyl 3-phenylpropionate **8** and subsequent mixed anhydride reduction of carboxylic acid **9** furnished target building block **1** (Scheme 1).

Scheme 1. Synthesis of core aldehyde building block **1**.
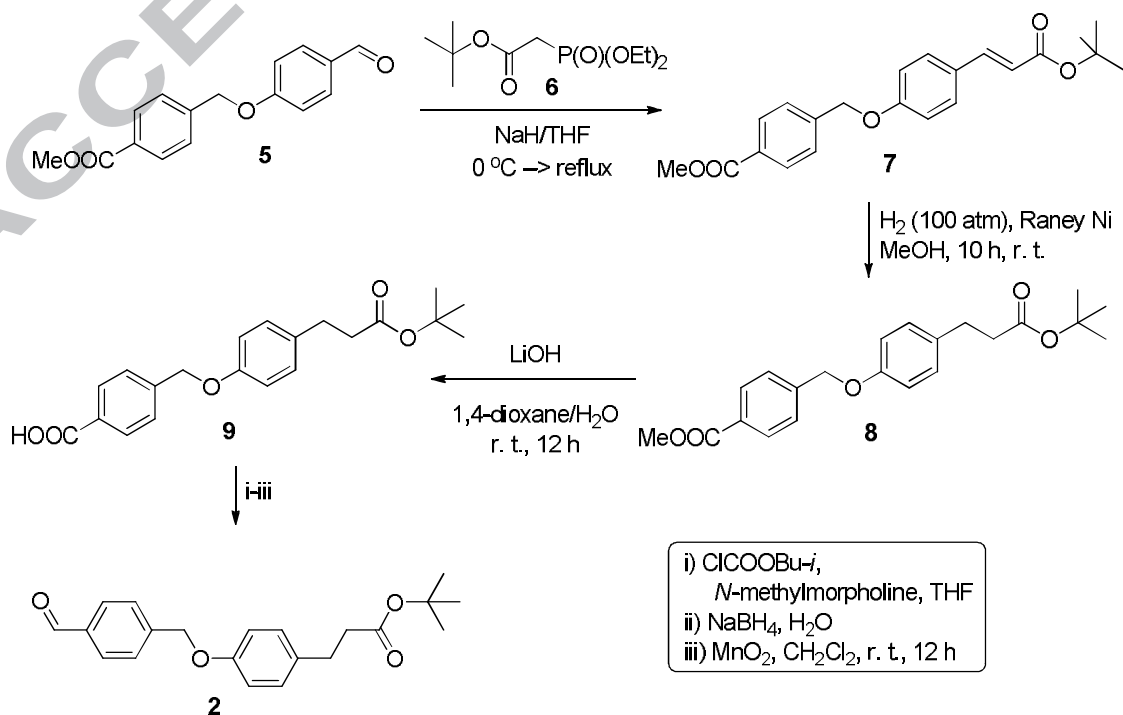
The diverse set of periphery spirocyclic building blocks **3a-r** was synthesized from progenitor **1** as summarized in Scheme 2. Sodium alkoxide, generated via treatment of **1** with sodium hydride in DMF, was alkylated with a set of alkyl halides to furnish, after Boc group removal, building blocks **3a-g**.

Multigram-scale oxidation of **1** with PDC furnished ketone **10** which served as a starting material for preparation of the rest of building blocks **3h-r**. The Wittig reaction of **10** with phosphonium ylides (generated by treatment of the respective phosphonium salts with *n*-BuLi) furnished respective olefins, all of which, except for unsubstituted methylene compound, were obtained as difficult-to-separate mixtures of *E*- and *Z*-isomers. After brief fractionation on silica gel, the olefin intermediates were hydrogenated over 10% Pd on carbon using ammonium formate as a source of hydrogen. Upon removal of the Boc group, a set of building blocks **3h-o** was obtained.

Considering the previous success in grafting polar heterocycles onto the periphery of FFA1 agonists,[8] we designed 1,2,4-oxadiazole containing spirocyclic piperidine building blocks **3p-r**. The synthesis of the latter was achieved via a multistep reaction sequence which included Horner-Wadsworth-Emmons olefination, reduction of the α,β-unsaturate ester, alkaline hydrolysis of its saturated counterpart to provide common carboxylic acid starting material **11**. Activation of the carboxylic functionality in the latter with isobutyl chloroformate followed by the reaction with the respective amidoximes, cyclodehydration of the resulting initial adducts on treatment with TBAF in refluxing toluene, and Boc group removal furnished target 1,2,4-oxadiazoles **3p-r** (Scheme 2).

Scheme 2. Synthesis of spirocyclic building blocks **3a-r**.
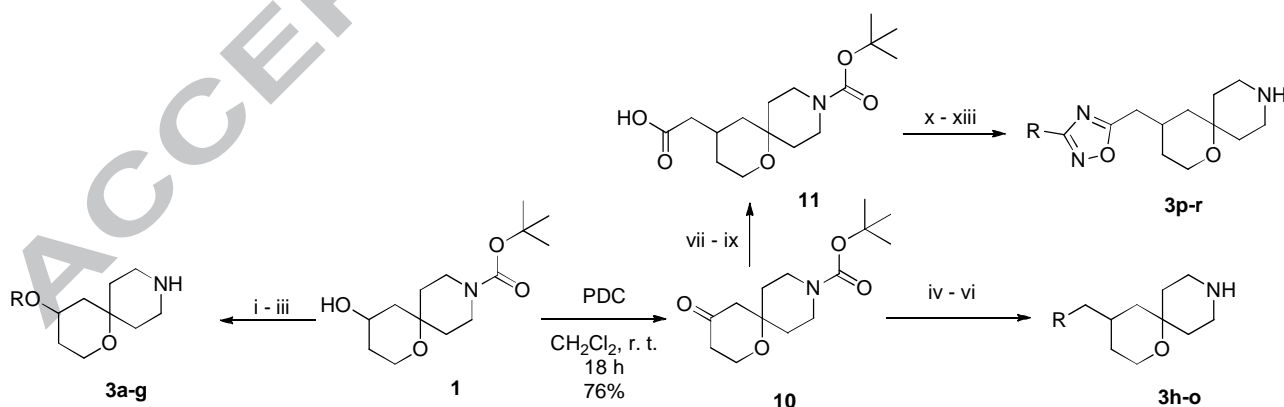
Reagents and conditions: i. NaH, DMF, 0 ℃, 30 min; ii. RHal, DMF, 0 ℃ → r. t., 18 h; iii. TFA, CH₂Cl₂, 0 ℃, 6 h; iv. RCH₂PPh₃Cl, *n*-BuLi, THF, 0 ℃ → r. t., 18 h; v. HCOONH₄, 10% Pd-C, EtOH, reflux, 12 h; vi. TFA, CH₂Cl₂, 0 ℃, 6 h; vii. EtOOCCH₂P(O)(OEt)₂, NaH, THF, 0 ℃ → r. t., 18 h; viii. HCOONH₄, 10% Pd-C, EtOH, reflux, 12 h; ix. KOH, aq. MeOH, r. t., 18 h; x. *i*-BuOOCCl, THF, *N*-methylmorpholine, -30 ℃, 30 min; xi. RC(NH₂)=NOH, r. t., 12 h; xii. TBAF, toluene, reflux, Dean-Stark trap; xiii. TFA, CH₂Cl₂, r. t. 18 h.

Spirocyclic building blocks **3a-r** thus synthesized (as well as commercially available unsubstituted 1-oxa-9-azaspiro[5.5]undecane **12**) were then employed in reductive amination of aldehyde **2** and, after brief fractionation of the tertiary amine products, the Boc protecting group was removed using TFA in CH_2Cl_2, followed by counter-ion exchange with HCl in diethyl ether, to furnish the target compounds **4a-s** (Scheme 3).

Scheme 3. Preparation of FFA1 agonists **4a-s** studied in this work.
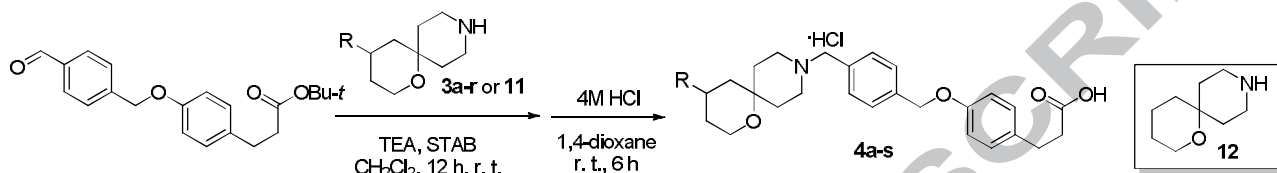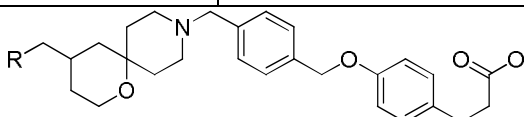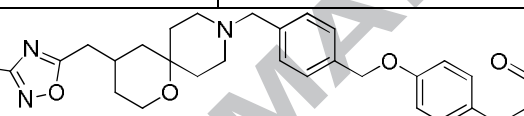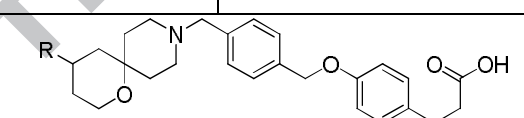
It should be noted that, owing to difficulties we faced in purification of the hydrochloride products, which required repeated manipulation of semi-purified material, the isolated yields of compounds **4a-s** achieved in this study were relatively low (see ESI). Nonetheless, the synthetic strategy described above allowed the preparation of the required quantities of compounds **4a-s** for the initial *in vitro* biological profiling of the lead compounds thus identified – for *in vitro* ADME and *in vivo* PK characterization. Further optimization of the synthesis of the frontrunner compounds will be needed before further development of the series disclosed herein.

Potential FFA1 agonists **4a-s** thus synthesized were tested for FFA1 activation using calcium flux assay employing Chinese hamster ovary (CHO) cells engineered to stably express human FFA1. All compounds were tested in dose-response (% FFA1 activation) mode in order to determined EC_{50} values. The latter, as well as % of maximum efficacy achieved for active compounds relative to reference agonist GW9508[16] (used at 5 μM concentration throughout the study) are given in Table 1.

Table 1. FFA1 agonists **4a-r** studied in this work.

Compound	R	FFA1 $EC_{50} \pm SD$, μM[a]	% efficacy[b]
4a	Me	>20.00	n/a
4b	Et	>20.00	n/a
4c		>20.00	n/a
4d	3-$FC_6H_4CH_2$	1.30 ± 0.24	98

4e	4-F$_3$CC$_6$H$_4$CH$_2$	>20.00	n/a
4f	PhCH$_2$	1.16 ± 0.12	100
4g	4-FC$_6$H$_4$CH$_2$	2.01 ± 0.52	75

4h	H	>20.00	n/a
4i	4-F$_3$CC$_6$H$_4$	1.27	74
4j	3-FC$_6$H$_4$	>20.00	n/a
4k	4-FC$_6$H$_4$	0.41 ± 0.07	88
4l	Ph	0.055 ± 0.011	93
4m	4-MeOC$_6$H$_4$	0.28 ± 0.04	100
4n	4-MeC$_6$H$_4$	0.077 ± 0.02	74
4o	2-FC$_6$H$_4$	0.81 ± 0.21	95

4p	3-Py	>20.00	n/a
4q	(cyclopropyl)—*	4.54 ± 0.73	53
4r	MeOCH$_2$CH$_2$	>20.00	n/a

4s	H	>20.00	n/a

[a] Each value is an average of $n = 4$.

[b] Relative to GW9508[16] (5 μM).

On examination of the FFA1 activation data presented in Table 1 it becomes clear that in the newly designed series, increased lipophilicity (in combination with the basic nitrogen center counter-balancing the lipophilic periphery) is the principal driver of potency, as it was described for FFA1 agonists in a number of instances.[10,17] This should be expected for receptors modulated by endogenous free fatty acids and for the ligands intended to mimic the lipophilic character of the latter. Indeed, the hydrophilicity imparted by unsubstituted 1-oxa-9-azaspiro[5.5]undecane periphery (compound **4s**) was detrimental to the agonistic potency. However, introduction of alkoxy substituents of increasing size (compound **4a-g**) gradually brought the potency back into low-micromolar range. Of particular interest is the influence of alkyl substituents in the pyran portion of

the new FFA1 agonist scaffold of the potency (exemplified by compounds **4h-o**). Here, introduction of lipohilic benzyl periphery results in a significant potency increase, with the most compound (**4l**) having EC_{50} comparable to that of Takeda's phase III compound TAK-875 ($EC_{50} = 0.014$ μM).[18] Taking into account the size of the pilot set of compounds studied in this work, this attests to the success of the initial FFA1 design idea implemented in the new molecular scaffold.

We next determined the selectivity profile of the most potent GPR40 agonists (**4k-n**) against other free fatty acid receptors (FFA3/GPR41, FFA2/GPR43 and FFA4/GPR120). FFA2 and FFA3 agonists have a preference in binding short-chain fatty acids while FFA1 and FFA4 have a higher affinity to medium- and long-chain fatty acids.[19,20] As it is seen from the activity data against this panel of GPCRs, the four lead compounds displayed high selectivity for FFA1 (Table 2).

Table 2. Selectivity profile for compounds **4k-n**.[a]

	4k	4l	4m	4n
human FFA1/GPR40 EC_{50} (μM)	0.41	0.055	0.28	0.077
human FFA3/GPR41 EC_{50} (μM)	>10	>10	>10	>10
human FFA2/GPR43 EC_{50} (μM)	>10	>10	>10	>10
human FFA4/GPR120 EC_{50} (μM)	>10	>10	>10	>10

[a] Each value is an average of n = 4 in the presence of 0.1% BSA.

In order to better understand the dramatic influence of the benzyl substituent in the 1-oxa-9-azaspiro[5.5]undecane portion of the compounds (compared to the unsubstituted derivative), we have docked **4l** and **4s** in the FFA1 binding site (Figure 3).
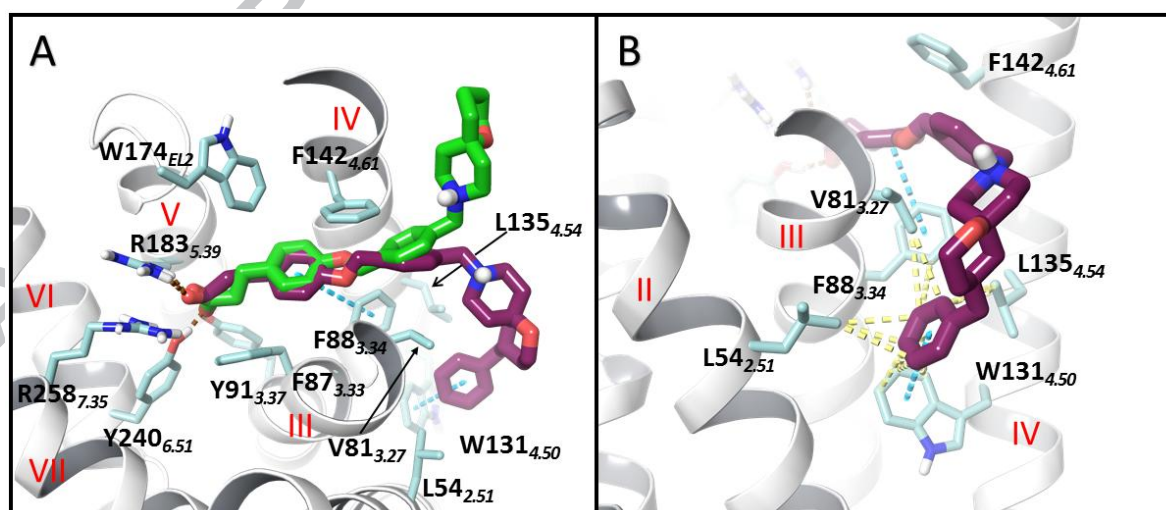
Figure 3. Docked poses of compounds **4l** and **4s** at FFA1. (A) Overlay of **4l** (maroon) and **4s** (green) in the FFA1 active site. (B) Hydrophobic interactions of the benzyl substituent. Protein-Ligand interactions are visualized for compound **4l** in A, only. Hydrogen bonds, π-π and hydrophobic interactions are in a brown, blue and yellow dashed-line, respectively. Each transmembrane helix is labeled in red roman numerals. Residues have been labeled with their position followed by the Ballesteros and Weinstein numbering[21] in subscript.

Both compounds occupy similar positions within the binding cativy, forming the critical hydrogen bonds with $R183_{5.39}$, $R258_{7.35}$, $Y91_{3.37}$ and $Y240_{6.51}$. The propanoic acid moeity may be further stabilized by a network of π- π interactions that could occur between $F88_{3.34}$, $F142_{4.61}$, $W174_{EL2}$ and $F87_{3.33}$ of the receptor and the aromatic rings of each compound. However, there are signifigant differences in the positioning of the spiro-pyran moiety, which is likely responsible for the observed differences in the potency of **4l** (EC_{50} = 0.055 μM) and **4s** (EC_{50} >20.00 μM). In **4s**, this moiety positions toward the extracellular side while, in contrast, the potent **4l** adopts a position, where 1-oxa-9-azaspiro[5.5]undecane faces toward the intercelluar side (Figure 3A). Here, the terminal benzyl substituent positions within a favorable hydrophobic cavity forming numerous hydrophobic interactioins with $L54_{2.51}$, $L135_{4.54}$ and $V81_{3.27}$,, while also having π- π stacking interactions with $W131_{4.50}$ (Figure 3B). Together these contacts drive the benzyl-substituted 1-oxa-9-azaspiro[5.5]undecane moiety deep into the phosopholipid bilayer, which might be benefical for agonist activity.
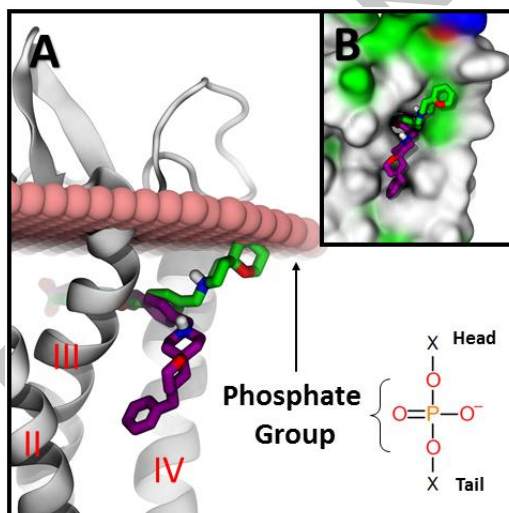
Figure 4. (A) Overlay of **4l** (maroon) and **4s** (green) in the FFA1 active site in the presence of the predicted position of the lipid bilayer demonstrated by the lipid phosphate groups in the form of pink spheres. (B) Surface representation of the FFA1 that interfaces with the lipid bilayer with the docking pose of **4l** (maroon) and **4s** (green). The surface colors: white, green, blue and red correspond to hydrophobic, hydrophilic, negatively charged and positively charged residues, respectively. Each transmembrane helix is labeled in red roman numerals.

To appreciate the positioning of the lipid bilayer and its possible interactions with the ligand tails, we used the Orientation of Proteins in Membrane (OPM) database and PPM webserver (REF: 27) to align and perdict the position of FFA1 in a membrane (Figure 4A). The position of **4s** within the binding cavity is seemlingly tolerable, however, the ligand stablity is likely compromised by the electrostatic interactions between the positively charged amonium of its spyrio-pyran motif and the negatively charged phospholipid head. Here, the fluidity of the lipid bi-layer coupled with these strong electrostatic interactions may destabalise the binding conformation, which likely attributes to the low activity of the compound. In contrast, the benzyl substituent of compound **4l** favors the

more hydrophobic environment (Figure 4B), positioning at the interface between the lipid tails and protein which negates the detrimental attraction between the phostphate heads and positively charged amonium.

Since we were able to reach well into submicromolar potency range with our pilot set of 19 compounds (**4a-s**), we were also keen on assessing the preliminary ADME profile of the most active compounds from this set (**4k-n**). On examination of the data presented in Table 3, several general observations can be made. All four compounds displayed satisfactory aqueous solubility and Caco-2 permeability, which confirmed the new chemotype was promising from further development prospective. The relatively high plasma protein binding observed for **4k-n** perhaps is not surprising for these highly lipophilic compounds[22] and may not present a significant development obstacle provided the rate of dissociation from plasma proteins is sufficient to maintain the required plasma levels (*vide infra*). The principal weakness of the series studied herein was its low metabolic stability determined by incubation of compounds **4k-n** in the presence of mouse liver microsomes. Indeed the half-life of **4l-m** was around 10 minutes with unacceptably high clearance. This could be attributed to the presence of two heteroatom-substituted benzylic positions or β-unsubstituted propanoic acid moiety, which could be prone to metabolic oxidation.[4]

Table 3. ADME profile of compounds **4k-n**.

		4k	4l	4m	4n
Aqueous solubility (PBS, pH 7.4)[a] (µM)		143	151	42	69
Plasma protein binding (human)[a] (%)		98.3	98.8	99.3	99.8
Metabolic stability (mouse liver microsomes)	$T_{1/2}$, min	23.4	8.5	11.8	9.6
	CL_{int}, µL/min/mg	71.3	196.0	141.1	173.3
A-B permeability (Caco-2, cm·s^{-1})[b] (·10^{-6})		8.7	12.0	15.8	10.4

[a] Each value is an average of n = 4, measured at c = 1 µM.
[b] Each value is an average of n = 2, measured at c = 10 µM.

The highest metabolic stability observed for compound **4k** (EC_{50} = 0.41 µM corresponding to 218 ng/mL) among the four selected frontrunner candidates was the principal decisive point in nominating this compounds for pharmacokinetic characterization in mice at the dosage of 10 mg/kg (administered intravenously and orally).

As can be seen from pharmacokinetic parameters presented in Table 4, compound **4k** demonstrated satisfactory oral bioavailability (F, %) and plasma levels commensurate with or significantly higher than the *in vitro* EC_{50} value, on oral and intravenous administration, respectively.

Table 4. Pharmacokinetic parameters determined in C57BL/6J mice (n=5 per treatment group).

	4k i.v. (10 mg/kg)	**4k** p.o. (10 mg/kg)
T_{max} (min)	10	30
C_{max} (ng/mL)	2,772	226
AUC_{inf_obs} (min·ng/mL)	107,519	11,055
F (%)	10.3	

3. Conclusions

The toxicity associated with high lipophilicity of previous FFA1 agonists has been a limiting factor in the progression through clinical trials. Here, we have reported on a novel series of FFA1 (GPR40) agonists. The series was designed based on the basic amine spirocyclic periphery motif present in Eli Lilly's advance FFA1 agonist LU2881835. A diverse set of 19 compounds was synthesized via decoration of the 3-[4-(benzyloxy)phenyl]propanoic acid core building block with a set of spirocyclic piperidines synthesized from Boc-protected 1-oxa-9-azaspiro[5.5]undecan-4-ol which, in turn, had been reported as amenable on multigram scale via Prins chemistry. The compounds displayed meaningful structure-activity relationships *in vitro* stimulating calcium flux in FFA1-overexpressing CHO cells and four frontrunner compounds having EC_{50} values in the 0.055 – 0.41 μM range have been identified. The compounds displayed an overall satisfactory profile except for low metabolic stability. Compound **4k** having the highest mouse liver microsome stability and EC_{50} = 0.41 μM was evaluated for pharmacokinetics in mice on intravenous and oral administration. This lead compound demonstrated high plasma levels achieved even on oral administration of 10 mg/kg dose and absolute oral bioavailability (F) of 10.3%. This compound represents a promising lead for further optimization and development of the novel class of therapies against type 2 diabetes mellitus.

4. Experimental section

4.1. General experimental

All reactions were conducted in oven-dried glassware in atmosphere of nitrogen. Melting points were measured with a Buchi B-520 melting point apparatus and were not corrected. Analytical thin-layer chromatography was carried out on Silufol UV-254 silica gel plates using appropriate mixtures of ethyl acetate and hexane. Compounds were visualized with short-wavelength UV light. ^{1}H NMR and ^{13}C NMR spectra were recorded on Bruker MSL-300 spectrometers in DMSO-D6-*d6* using TMS as an internal standard. Mass spectra were recorded using Shimadzu LCMS-2020

system with electron-spray (ESI) ionization. All and reagents and solvents were obtained from commercial sources and used without purification.

All mass-spectroscopic measurements required for determination of ADME properties were performed using Shimadzu VP HPLC system including vacuum degasser, gradient pumps, reverse phase HPLC column, column oven and autosampler. The HPLC system was coupled with tandem mass spectrometer API 3000 (PE Sciex). The TurboIonSpray ion source was used in both positive and negative ion modes. Acquisition and analysis of the data were performed using Analyst 1.5.2 software (PE Sciex).

4.2. Synthetic organic chemistry

4.2.1. Starting materials

Boc-protected 1-oxa-9-azaspiro[5.5]undecan-4-ol (**1**) was synthesized as described previously.[14] 1-oxa-9-azaspiro[5.5]undecane (**12**) is a commercially available compound which can, alternatively, be prepared by deprotection of its *N*-Boc version reported earlier.[14] Aldehyde **5** is a known compound prepared according to the literature protocol.[15]

4.2.1.1. Methyl 4-({4-[(1*E*)-3-*tert*-butoxy-3-oxoprop-1-en-1-yl]phenoxy}methyl)benzoate (7).

A 500-mL round-bottomed flask was charged with a suspension of NaH (60% dispersion in mineral oil, 1.1 g, 28 mmol) in dry THF (250 mL) and cooled to 0 °C. Phosphonate **6** (7.6 g, 30 mmol) was added in portions and the resulting mixture was stirred at that temperature for 1 h. A solution of compound **5** (6.7 g, 25 mmol) in THF (50 mL) was added dropwise. The reaction mixture was heated at reflux for 30 min, cooled down to r. t. and poured into water (250 mL). The aqueous solution was extracted with ethyl acetate (3 x 100 mL) and the combined organic extracts were washed with 5% aqueous HCl, 10% aqueous potassium bicarbonate, water, dried over anhydrous Na$_2$SO$_4$, filtered and concentrated *in vacuo*. The residue was purified by column chromatography on silica gel using 0→15% ethyl acetate in hexanes as eluent to provide the title compound. Yield 7.7 g (21 mmol, 83%); white crystals; mp = 104-107 °C; ^{1}H NMR (300 MHz, CDCl$_3$) δ 8.07 (d, *J* = 8.2 Hz, 2H), 7.60 – 7.43 (m, 5H), 6.96 (d, *J* = 8.7 Hz, 2H), 6.26 (dd, *J* = 15.9, 2.5 Hz, 1H), 5.15 (s, 2H), 3.93 (d, *J* = 2.4 Hz, 3H), 1.54 (s, 9H); ^{13}C NMR (75 MHz, DMSO) δ 166.8, 166.6, 159.9, 143.0, 141.7, 129.9, 129.6, 127.9, 127.0, 118.1, 115.1, 80.3, 69.4, 52.2, 28.2; MS *m/z* 369.6 (M + H$^+$).

4.2.1.2. Methyl 4-{[4-(3-*tert*-butoxy-3-oxopropyl)phenoxy]methyl}benzoate (8).

A 500-mL autoclave chamber was charged with a solution of compound **7** (7.7 g, 21 mmol) anhydrous methanol (250 mL) and Raney Ni (10 g, freshly prepared suspension). A 100-atm pressure of hydrogen was applied and the mixture was stirred at r. t. for 10 h. Upon release of the

hydrogen pressure and purging with nitrogen, the contents of the autoclave were filtered through a pad of celite, washed with methanol and the filtrate was concentrated *in vacuo* to provide the title compound.

Yield 7.8 g (21 mmol, quantitative); white crystals, mp = 62-64 °C; ^{1}H NMR (300 MHz, CDCl$_3$) δ 8.08 (t, *J* = 10.6 Hz, 2H), 7.51 (d, *J* = 8.1 Hz, 2H), 7.13 (d, *J* = 8.5 Hz, 2H), 6.89 (d, *J* = 8.5 Hz, 2H), 5.12 (s, 2H), 3.93 (s, 3H), 2.86 (t, *J* = 7.7 Hz, 2H), 2.51 (t, *J* = 7.7 Hz, 2H), 1.43 (s, 9H); ^{13}C NMR (75 MHz, MeOD) δ 172.3, 166.9, 156.9, 142.4, 133.5, 129.9, 129.6, 129.4, 127.0, 114.8, 80.3, 69.4, 52.2, 37.3, 30.3, 28.1; MS *m/z* 371.5 (M + H^{+}).

4.2.1.3. 4-{[4-(3-*Tert*-butoxy-3-oxopropyl)phenoxy]methyl}benzoic acid (9).

A 25-mL round-bottomed flask was charged with a solution of compound 8 (2.7 g, 7.29 mmol) in 1,4-dioxane (15 mL). A solution of LiOH (170 mg, 7.29 mmol) in water (3.0 mL) was added and the resulting mixture was stirred at r. t. for 12 h. 1,4-Dioxane was removed in vacuo and the residue was dissolved in water (100 mL). The aqueous solution was extracted with ethyl acetate (3 x 50 mL) and the organic extracts were discarded. The pH of the aqueous phase was carefully adjusted to 5.0 with 5% aqueous HCl and the solution was again extracted with ethyl acetate (3x50 mL). The combined organic extracts were dried over anhydrous Na$_2$SO$_4$, filtered and concentrated *in vacuo*. The residue was purified by column chromatography on silica gel using 0→5% methanol in chloroform. The analytically pure title compound was obtained after crystallization from toluene.

Yield 1.8 g (5.1 mmol, 70%); white crystals, mp = 173-175 °C; ^{1}H NMR (300 MHz, CDCl$_3$) δ 8.13 (d, *J* = 8.2 Hz, 2H), 7.54 (d, *J* = 8.2 Hz, 2H), 7.13 (d, *J* = 8.5 Hz, 2H), 6.89 (d, *J* = 8.5 Hz, 2H), 5.13 (s, 2H), 2.86 (t, *J* = 7.7 Hz, 2H), 2.51 (t, *J* = 7.7 Hz, 2H), 1.41 (s, 9H); ^{13}C NMR (75 MHz, CDCl$_3$) δ 172.4, 171.8, 156.8 143.5, 133.5, 130.5, 129.4, 128.7, 127.0, 114.8, 80.4, 69.3, 37.3, 30.3, 28.1; MS *m/z* 357.6 (M + H^{+}).

4.2.1.4. *Tert*-butyl 3-{4-[(4-formylbenzyl)oxy]phenyl}propanoate (1).

A 250-mL three-necked round-bottomed flask kept under a positive pressure of nitrogen was charged with a solution of compound **9** (5.3 g, 15 mmol, obtained from several runs of the previous three steps) in anhydrous THF (100 mL) and *N*-methylmorpholine (1.7 g, 17 mmol). The mixture was cooled to -30 °C and a solution of isobutyl chloroformate (2.3 g, 17 mmol) in anhydrous THF (10 mL) was added dropwise. The reaction mixture temperature was allowed to reach -5 °C and the precipitate formed was filtered off. To the filtrate thus obtained, a suspension of sodium borohydride (1.1 g, 5.61 mmol) in water (10 mL) was added in portions. The resulting mixture was stirred for 30 min. The volatiles were removed in vacuo and the residue was partitioned between

ethyl acetate (200 mL) and water (100 mL). The organic layer was washed with 5% aqueous HCl, 5% aqueous potassium carbonate and brine, dried over anhydrous Na_2SO_4, filtered and concentrated in vacuo. The residue (5.0 g) was dissolved in dichloromethane (50 mL) and active MnO_2 (15 g) was added. The resulting mixture was stirred at r. t. for 12 h, filtered through a pad of celite and the latter was washed with copious amounts of dichloromethane. The filtrate was concentrated *in vacuo*. The residue was purified by column chromatography on silica gel using 0→10% ethyl acetate in hexanes as eluent to provide the title compound.

Yield 3.1 g (9.0 mmol, 60.7% over 2 steps); white crystals, mp = 57-59 °C; ^{1}H NMR (300 MHz, DMSO) δ 10.03 (s, 1H), 7.91 (d, *J* = 8.1 Hz, 2H), 7.61 (d, *J* = 8.0 Hz, 2H), 7.14 (d, *J* = 8.5 Hz, 2H), 6.90 (d, *J* = 8.6 Hz, 2H), 5.14 (s, 2H), 2.87 (t, *J* = 7.7 Hz, 2H), 2.52 (t, *J* = 7.7 Hz, 2H), 1.42 (s, 9H); ^{13}C NMR (75 MHz, $CDCl_3$) δ 191.9), 172.3, 156.7, 144.2, 135.9, 133.6, 130.0, 129.4, 127.5, 114.8, 80.3, 69.2, 37.3, 30.3, 28.1; MS *m/z* 341.4 (M + H^{+}).

4.2.1.5. *tert*-Butyl 4-oxo-1-oxa-9-azaspiro[5.5]undecane-9-carboxylate (10).

To a solution of **1** (47.0 g, 173 mmol) in dichloromethane (500 mL) PDC (130 g, 346 mmol) was added in small portions. The reaction mixture was stirred at r. t. for 18 h. The precipitate formed was filtered off and washed with dichloromethane (150 mL). The combined filtrate and washings were washed with 5% aqueous HCl, dried over anhydrous Na_2SO_4, filtered and concentrated *in vacuo*. The residue was purified by column chromatography on silica gel using chloroform as eluent to provide the title compound.

Yield 35.4 g (131 mmol, 76%). White crystalline solid, m. p. = 61 – 64 ºC. ^{1}H NMR (300 MHz, DMSO-d_6) δ 4.00 (t, *J* = 6.1 Hz, 2H), 3.75 (dd, *J* = 10.1, 3.3 Hz, 2H), 3.22 – 3.09 (m, 2H), 2.46 (t, *J* = 6.0 Hz, 2H), 2.36 (s, 2H), 1.80 (d, *J* = 12.9 Hz, 2H), 1.50 (dd, *J* = 14.6, 2.8 Hz, 2H), 1.45 (s, 9H). ^{13}C NMR (75 MHz, DMSO-d_6) δ 206.8, 154.8, 79.6, 74.9, 60.4, 52.7, 41.7, 39.1, 34.4, 28.4. MS *m/z* 270.2 (M+H^{+}).

4.2.1.6. 2-(9-(*tert*-Butoxycarbonyl)-1-oxa-9-azaspiro[5.5]undecan-4-yl)acetic acid (11).

To a 0 ºC, vigorously stirred suspension of NaH (6.54 g, 163 mmol, 60% dispersion in mineral oil) in THF (300 mL) thriethylphosphonoacetate (45 g, 200 mmol) was added dropwise under argon. The stirring continued at that temperature for 1 h, whereupon a solution of **10** (40 g, 149 mmol) in THF (100 mL) was added. The reaction mixture was allowed to reach r. t. and was stirred at that temperature for 18 h. The reaction mixture was poured into water (500 mL) and the aqueous phase was extracted with ethyl acetate (3 x 200 mL). The combined organic extracts wer washed with 3% aqueous citric acid, 5% aqueous $NaHCO_3$, brine, dried over anhydrous Na_2SO_4, filtered and

concentrated *in vacuo*. The residue was fractionated on silica gel using 0→5% ethyl acetate in hexanes as eluent. The fractions containing the olefination product (according to LC MS analysis) were pooled and concentrated to dryness (yielding 32.7 g of the material). The residue (10.9 g) was dissolved in EtOH (200 mL), HCOONH$_4$ (2.8 g, 0.44 mmol) and 10% Pd on carbon (300 mg) were added and the resulting mixture was heated at reflux for 12 h. The mixture was cooled to r. t. and filtered through a plug of Celite (subsequently washing the latter with EtOH). The combined filtrate and washings were concentrated to dryness. The residue was partitioned between water (150 mL) and ethyl acetate (150 mL). The organic layer was separated and the aqueous layer was additionally extracted with ethyl acetate (2 x 150 mL). The combined organic extracts were washed with 3% aqueous citric acid, 5% aqueous NaHCO$_3$ and brine, dried over anhydrous Na$_2$SO$_4$, filtered and concentrated *in vacuo*. The residue was dissolved in MeOH (100 mL) and a solution of KOH (5.42 g, 96.7 mmol) in water (20 mL) was added. The mixture was stirred at r. t. for 18 h and concentrated to dryness *in vacuo*. The residue was dissolved in water (100 mL), the aqueous solution was extracted with ether (2 x 50 mL) and then acidified to pH 5.0 with 3% aqueous HCl. The solution thus obtained was extracted with ethyl acetate (3 x 100 mL) and the combined organic extracts were washed with brine, dried over anhydrous Na$_2$SO$_4$, filtered and concentrated *in vacuo* to provide analytically pure **11**.

Yield 7.35 g (49%). ^{1}H NMR (300 MHz, DMSO-*d$_6$*) δ 12.03 (s, 1H), 3.67 – 3.45 (m, 4H), 3.16 – 2.83 (m, 2H), 2.16 – 1.95 (m, 4H), 1.63 – 1.51 (m, 2H), 1.49 – 1.30 (m, 2H), 1.38 (s, 9H), 1.28 – 0.89 (m, 3H). ^{13}C NMR (75 MHz, DMSO-*d$_6$*) δ 173.2, 153.9, 78.4, 69.7, 59.7, 41.6, 41.1, 38.6, 32.0, 28.7, 28.1, 26.8. MS *m/z* 314.5 (M+H$^+$).

4.2.2. General procedure for the preparation of compounds 3a-g.

A solution of *tert*-butyl 1-oxa-9-azaspiro[5.5]undecan-4-ol (4g, 14.8 mmol) in DMF (20 mL) was added dropwise to a 0 ºC suspension of NaH (1.3 g, 32.6 mmol, 60% dispersion in mineral oil) in dry DMF (100 mL) under argon. The resulting mixture was stirred at 0 ºC for 30 min whereupon a solution of the respective alkyl halide - MeI, EtBr, *cyclo*-PrCH$_2$Br or ArCH$_2$Cl (19.2 mmol) – in DMF (10 mL) was added dropwise. The resulting mixture was allowed to warm up to r. t. and stirred at that temperature for 18 h. The reaction mixture was poured into water (200 mL) and the aqueous phase was extracted with ethyl acetate (3 x 200 mL). The combined organic extracts were washed with 3% aqueous citric acid, 5% aqueous NaHCO$_3$, brine and water, dried over anhydrous Na$_2$SO$_4$, filtered and concentrated *in vacuo*. The residue was fractionated on silica gel using 0 →5% ethyl acetate in hexanes as eluent and the fractions containing the desired product (according to LC MS analysis) were combined and concentrated in dryness. Without further purification, the residue

was dissolved in CH_2Cl_2 (3 mL/mmol calculated assuming 100% purity of the material obtained in the previous step), the solution was cooled to 0 ℃ and TFA (1 mL/mmol) was added. The mixture thus obtained was stirred at 0 ℃ for 6 h and then concentrated to dryness to provide, after crystallization from isopropyl alcohol, the target spirocyclic piperidine as a trifluoroacetate salt. Compounds **3a-b** were converted to hydrochloride salts by treatment of their r. t. solutions in 1,4-dioxane with 4M HCl in 1,4-dioxane followed by stirring for 3 h, evaporation of the volatiles *in vacuo* and crystallization from isopropyl alcohol.

4.2.2.1. 4-Methoxy-1-oxa-9-azaspiro[5.5]undecane hydrochloride (3a).

Yield 1.16 g (75%). White crystals, m. p. = 188 – 191 ℃. ^{1}H NMR (300 MHz, DMSO-d_6) δ 9.02 (s, 1H), 8.98 (s, 1H), 3.78 – 3.67 (m, 1H), 3.55 – 3.35 (m, 2H), 3.23 (s, 3H), 3.06 – 2.76 (m, 4H), 2.11 – 2.02 (m, 1H), 1.91 – 1.55 (m, 5H), 1.38 – 1.16 (m, 2H). ^{13}C NMR (75 MHz, DMSO-d_6) δ 71.9, 69.1, 58.3, 54.8, 40.4, 38.8, 33.5, 31.3, 28.0. MS *m/z* 185.9 (M+H^{+}).

4.2.2.2. 4-Ethoxy-1-oxa-9-azaspiro[5.5]undecane hydrochloride (3b).

Yield 991 mg (63%). White crystals, m. p. = 191 – 193 ℃. ^{1}H NMR (300 MHz, DMSO-d_6) δ 9.04 (s, 1H), 8.94 (s, 1H), 3.76 – 3.55 (m, 2H), 3.54 - 3.49 (m, 1H), 3.44 (q, *J* = 7.00 Hz, 2H), 3.08 – 2.75 (m, 4H), 2.13 – 2.01 (m, 1H), 1.89 – 1.55 (m, 5H), 1.39 – 1.15 (m, 2H), 1.08 (t, *J* = 7.00 Hz, 3H). ^{13}C NMR (75 MHz, DMSO-d_6) δ 70.2, 69.1, 62.2, 58.4, 40.9, 38.8, 33.5, 31.9, 28.0, 15.6. MS *m/z* 199.8 (M+H^{+}).

4.2.2.3. 4-(Cyclopropylmethoxy)-1-oxa-9-azaspiro[5.5]undecane trifluoroacetate (3c).

Yield 1.29 g (62%). Hygroscopic solid. ^{1}H NMR (300 MHz, DMSO-d_6) δ 8.55 (s, 1H), 8.45 (s, 1H), 3.78 – 3.57 (m, 2H), 3.54 – 3.43 (m, 1H), 3.29 – 3.18 (m, 2H), 3.14 – 2.79 (m, 4H), 2.19 – 1.48 (m, 6H), 1.40 – 1.20 (m, 2H), 1.01 – 0.88 (m, 1H), 0.48 – 0.38 (m, 2H), 0.17 – 0.09 (m, 2H). ^{13}C NMR (75 MHz, DMSO-d_6) δ 71.5, 70.2, 69.1, 58.5, 40.9, 39.1, 33.7, 32.0, 28.2, 11.0, 3.0, 2.9. MS *m/z* 226.3 (M+H^{+}).

4.2.2.4. 4-[(3-Fluorobenzyl)oxy]-1-oxa-9-azaspiro[5.5]undecane (3d).

This compound was converted to free base by partitioning between sat. aq. $NaHCO_3$ and ethyl acetate, followed by separation of ethyl acetate solution, drying over anhydrous Na_2SO_4, filtration, concentration *in vacuo* and flash chromatography on silica gel using 20% MeOH in CH_2Cl_2. Yield 940 mg (45%). ^{1}H NMR (300 MHz, CDCl3) δ 7.32 – 7.27 (m, 1H), 7.09 – 6.92 (m, 3H), 4.51 (s, 2H), 3.88 – 3.80 (m, 1H), 3.75 – 3.66 (m, 1H), 3.59 – 3.49 (m, 1H), 3.39 – 2.98 (m, 4H), 2.07 –

1.40 (m, 8H). ^{13}C NMR (75 MHz, CDCl3) δ 162.9 (d, J = 245.8 Hz), 141.0 (d, J = 7.1 Hz), 129.9 (d, J = 8.1 Hz), 122.7 (d, J = 2.8 Hz), 114.4 (d, J = 24.1 Hz), 114.1 (d, J = 24.4 Hz), 77.2, 71.1, 69.9, 58.6, 41.1, 40.2, 40.0, 34.8, 31.7. MS m/z 279.9 (M+H$^+$).

4.2.2.5. 4-{[4-(Trifluoromethyl)benzyl]oxy}-1-oxa-9-azaspiro[5.5]undecane trifluoroacetate (3e).

Yield 1.40 g (68%). Hygroscopic solid. ^{1}H NMR (300 MHz, DMSO-d_6) δ 8.49 (s, 2H), 7.68 (d, J = 8.09 Hz, 2H), 7.53 (d, J = 8.00 Hz, 2H), 4,60 (s, 2H) , 3.79 – 3.72 (m, 2H), 3.55 – 3.47 (m, 1H), 3.10 – 2.82 (m, 4H), 2.08 – 2.02 (m, 1H), 1.93 – 1.31 (m, 7H). ^{13}C NMR (75 MHz, DMSO-d_6) δ 144.0, 128.0 (q, J = 31.8 Hz), 127.7, 125.2 (q, J = 3.63 Hz), 124.4 (q, J = 271.8 Hz), 70.9, 69.2, 68.1, 58.4, 40.8, 39.1, 33.6, 31.8, 28.4. MS m/z 330.2 (M+H$^+$).

4.2.2.6. 4-(Benzyloxy)-1-oxa-9-azaspiro[5.5]undecane (3f).

This compound was converted to free base by partitioning between sat. aq. NaHCO$_3$ and ethyl acetate, followed by separation of ethyl acetate solution, drying over anhydrous Na$_2$SO$_4$, filtration, concentration *in vacuo* and flash chromatography on silica gel using 20% MeOH in CH$_2$Cl$_2$. Yield 1.50 g (75%). ^{1}H NMR (300 MHz, DMSO-d_6) δ 7.39 – 7.25 (m, 5H), 4.56 – 4.46 (m, 2H), 3.80 – 3.69 (m, 2H), 3.57 – 3.46 (m, 1H), 3.10 – 2.80 (m, 4H), 2.07 – 1.97 (m, J = 14.7 Hz, 1H), 1.96 – 1.80 (m, 3H), 1.74 – 1.26 (m, 4H). ^{13}C NMR (75 MHz, DMSO-d_6) δ 138.9, 128.2, 127.4, 127.3, 70.4, 69.3, 68.9, 58.3, 40.8, 39.3, 33.9, 31.8, 28.6. MS m/z 262.0 (M+H$^+$).

4.2.2.7. 4-[(4-fluorobenzyl)oxy]-1-oxa-9-azaspiro[5.5]undecane trifluoroacetate (3g).

Yield 930 mg (45%). Hygroscopic solid. ^{1}H NMR (300 MHz, DMSO-d_6) δ 8.57 (s, 1H), 8.38(s, 1H), 7.39 – 7.33 (m, 2H), 7.18 – 7.12 (m, 2H), 4.48 (s, 2H), 3.78 – 3.70 (m, 2H), 3.56 – 3.45 (m, 1H), 3.11 – 2.82 (m, 4H), 2.09 – 2.01 (m, 1H), 1.92 – 1.82 (m, 3H), 1.72 – 1.36 (m, 4H). ^{13}C NMR (75 MHz, DMSO-d_6) δ 161.5 (d, J = 242.9 Hz), 135.2 (d, J = 2.8 Hz), 129.5 (d, J = 8.1 Hz), 114.0 (d, J = 21.3 Hz), 70.5, 69.1, 68.2, 58.4, 40.8, 39.1, 33.6, 31.8, 28.3. MS m/z 279.8 (M+H$^+$).

4.2.3. General procedure for the preparation of compounds 3h-o.

n-BuLi (2.5M in hexane, 4 mL, 10.0 mmol) was added dropwise under argon to a 0 ºC suspension of the respective alkylphosphonium chloride (10.0 mmol) in THF (50 mL). The mixture was stirred for 30 min whereupon a solution of **10** (2.42 g, 9.0 mmol) in THF (10 mL) was added. The reaction mixture was allowed to warn up to r. t. and stirred at that temperature for 18 h. At that point, sat. aq. NH$_4$Cl (25 mL) was added and the mixture was diluted with ethyl acetate (50 mL) and water (20

mL). Organic phase was separated and the aqueous phase was additionally extracted with ethyl acetate (2 x 50 mL). The combined organic extracts were washed with brine, dried over anhydrous Na_2SO_4, filtered and concentrated *in vacuo*. The residue was fractionated on silica gel using 0→5% ethyl acetate in hexanes as eluent. Fractions containing the olefination product (according to LC MS analysis) were pooled and concentrated to dryness. The material thus obtained was used in the subsequent steps without further purification.

To a solution of this material in EtOH (20 mL/mmol assuming 100% purity of the product in the previous step) $HCOONH_4$ (4 mmol/mmol) and 10% Pd on carbon (37 mg/mmol) were added and the resulting mixture was heated at reflux for 12 h. The mixture was cooled to r. t. and filtered through a plug of Celite (subsequently washing the latter with EtOH). The combined filtrate and washings were concentrate to dryness. The residue was partitioned between water (50 mL) and ethyl acetate (50 mL). The organic layer was separated and the aqueous layer was additionally extracted with ethyl acetate (2 x 50 mL). The combined organic extracts were washed with 3% aqueous citric acid, 5% aqueous $NaHCO_3$ and brine, dried over anhydrous Na_2SO_4, filtered and concentrated *in vacuo*. Without further purification, the residue was dissolved in CH_2Cl_2 (3 mL/mmol calculated assuming 100% purity of the material obtained in the previous step), the solution was cooled to 0 ºC and TFA (1 mL/mmol) was added. The mixture thus obtained was stirred at 0 ºC for 6 h and then concentrated to dryness to provide, after crystallization from isopropyl alcohol, the target spirocyclic piperidine as a trifluoroacetate salt. Compounds **3h**, **3j**, **3m-n** were converted to hydrochloride salts by treatment of their r. t. solutions in 1,4-dioxane with 4M HCl in 1,4-dioxane followed by stirring for 3 h, evaporation of the volatiles *in vacuo* and crystallization from isopropyl alcohol.

4.2.3.1. 4-Methyl-1-oxa-9-azaspiro[5.5]undecane hydrochloride (3h).

Yield 342 mg (45%). White crystalline solid, m. p. = 223 – 226 ºC. ^{1}H NMR (300 MHz, DMSO-d_6) δ 9.07 (s, 1H), 9.03 (s, 1H) 3.71 – 3.45 (m, 2H), 3.06 – 2.90 (m, 3H), 2.87 – 2.72 (m, 1H), 2.36 – 2.26 (m, 1H), 1.80 – 1.70 (m, 2H), 1.59 – 1.45 (m, 4H), 1.11 – 0.90 (m, 2H), 0.85 (d, *J* = 6.41 Hz, 3H). ^{13}C NMR (75 MHz, DMSO-d_6) δ 68.2, 60.2, 43.8, 35.2, 34.1, 25.4, 24.3, 22.3. MS *m/z* 170.0 (M+H$^+$).

4.2.3.2. 4-[4-(Trifluoromethyl)benzyl]-1-oxa-9-azaspiro[5.5]undecane trifluoroacetate (3i).

Yield 1 g (38%). Hygroscopic solid. ^{1}H NMR (300 MHz, DMSO-d_6) δ 8.52 (s, 1H), 8.30 (s, 1H), 7.65 (d, *J* = 8.00 Hz, 2H), 7.42 (d, *J* = 7.92 Hz, 2H), 3.68 – 3.61 (m, 1H), 3.48 – 3.40 (m, 1H), 3.09 – 2.77 (m, 4H), 2.64 – 2.51 (m, 2H), 2,36 – 2.32 (m, 1H), 2.03 – 1.92 (m, 1H), 1.70 – 1.02 (m, 7H).

^{13}C NMR (75 MHz, DMSO-d_6) δ 144.8, 129.8, 126.7 (q, J = 31.6 Hz), 125.0 (q, J = 3.81 Hz), 122.6, 79.2, 68.1, 60.0, 42.2, 41.7, 35.3, 31.7, 31.1, 25.5. MS *m/z* 314.0 (M+H$^+$).

4.2.3.3. 4-(3-Fluorobenzyl)-1-oxa-9-azaspiro[5.5]undecane hydrochloride (3j)

Yield 1.03 g (65%). Hygroscopic solid. ^{1}H NMR (300 MHz, DMSO-d_6) δ 8.52 (s, 1H), 8.31 (s, 1H), 7.36 – 7.24 (m, 1H), 7.06 – 6.97 (m, 3H), 3.68 – 3.60 (m, 1H), 3.48 – 3.39 (m, 1H), 3.08 – 2.75 (m, 4H), 2.49 – 2.41 (m, 2H), 2.36 – 2.31 (m, 1H), 2.02 – 1.88 (m, 1H), 1.70 – 1.27 (m, 5H), 1.18 – 0.98 (m, 2H). ^{13}C NMR (75 MHz, DMSO-d_6) δ 162.2 (d, *J* = 242.9 Hz), 142.7 (d, *J* = 7.4 Hz), 130.0 (d, *J* = 8.3 Hz), 125.2, 115.6 (d, *J* = 20.5 Hz), 112.7 (d, *J* = 20.7 Hz), 68.1, 60.0, 42.2, 41.8, 35.3, 31.7, 31.0, 25.5. MS *m/z* 264.6 (M+H$^+$).

4.2.3.4. 4-(4-Fluorobenzyl)-1-oxa-9-azaspiro[5.5]undecane trifluoroacetate (3k)

Yield 1.02 g (81%). Hygroscopic solid. ^{1}H NMR (300 MHz, DMSO-d_6) δ 8.52 (s, 1H), 8.30 (s, 1H), 7.22 – 7.16 (m, 2H), 7.08 (t, *J* = 8.87 Hz, 2H), 3.66 – 3.60 (m, 1H), 3.47 – 3.38 (m, 1H), 3.09 – 2.98 (m, 3H), 2.89 – 2.75 (m, 1H), 2.44 (t, *J* = 7.23 Hz, 2H), 2.36 – 2.29 (m, 1H), 1.97 – 1.85 (m, 1H), 1.71 – 1.29 (m, 5H), 1.18 – 0.97 (m, 2H). ^{13}C NMR (75 MHz, DMSO-d_6) δ 160.8 (d, *J* = 241.1 Hz), 135.8 (d, *J* = 3.1 Hz), 130.7 (d, *J* = 7.7 Hz), 114.9 (d, *J* = 20.7 Hz), 68.2, 60.1, 41.8, 41.8, 35.4, 31.8, 31.4, 25.6. MS *m/z* 264.1 (M+H$^+$).

4.2.3.5. 4-Benzyl-1-oxa-9-azaspiro[5.5]undecane trifluoroacetate (3l)

Yield 1.03 g (74%). Hygroscopic solid. ^{1}H NMR (300 MHz, DMSO-d_6) δ 8.51 (s, 1H), 8.28 (s, 1H), 7.32 – 7.13 (m, 5H), 3.64 (dd, *J* = 11.75, 4.32 Hz, 1H), 3.43 (t, *J* = 11.30 Hz, 1H), 3.11 – 2.73 (m, 4H), 2.45 (t, *J* = 6.55 Hz, 2H), 2.38 – 2.29 (m, *J* = 14.72 Hz, 1H), 2.01 – 1.84 (m, 1H), 1.70 – 1.23 (m, 5H), 1.18 – 0.97 (m, 2H). ^{13}C NMR (75 MHz, DMSO-d_6) δ 139.7, 129.0, 128.2, 125.9, 68.1, 60.1, 42.7, 41.9, 35.4, 31.9, 31.3, 25.5. MS *m/z* 246.2 (M+H$^+$).

4.2.3.6. 4-(4-Methoxybenzyl)-1-oxa-9-azaspiro[5.5]undecane-9 hydrochloride (3m)

Yield 660 mg (62%). White crystalline solid, m. p. = 208 – 216 ºC. ^{1}H NMR (300 MHz, DMSO-d_6) δ 9.15 (s, 2H), 7.07 (d, *J* = 8.53 Hz, 2H), 6.83 (d, *J* = 8.54 Hz, 2H), 3.71 (s, 3H), 3.63 (dd, *J* = 11.73, 4.32 Hz, 1H), 3.49 – 3.37 (m, 1H), 3.04 – 2.70 (m, 4H), 2.39 (d, *J* = 6.94 Hz, 2H), 2.35 – 2.25 (m, 1H), 1.95 – 1.67 (m, 2H), 1.59 – 1.36 (m, 4H), 1.18 – 0.92 (m, 2H). ^{13}C NMR (75 MHz, DMSO-d_6) δ 157.4, 131.4, 129.8, 113.5, 68.1, 60.0, 54.8, 41.7, 38.8, 38.7, 35.1, 31.9, 31.3, 25.2. MS *m/z* 275.8 (M+H$^+$).

4.2.3.7. 4-(4-Methylbenzyl)-1-oxa-9-azaspiro[5.5]undecane hydrochloride (3n)

Yield 700 mg (53%). White crystalline solid, m. p. = 194 – 197 ºC. ^{1}H NMR (300 MHz, DMSO-d_6) δ 9.04 (s, 2H), 7.06 (q, J = 8.10 Hz, 4H), 3.64 (dd, J = 11.78, 4.33 Hz, 1H), 3.49 – 3.38 (m, 1H), 3.05 – 2.70 (m, 4H), 2.41 (d, J = 6.97 Hz, 2H), 2.26 (s, 3H), 1.97 – 1.83 (m, 1H), 1.80 – 1.35 (m, 6H), 1.18 – 0.93 (m, 2H). ^{13}C NMR (75 MHz, DMSO-d_6) δ 136.4, 134.6, 128.7, 128.6, 68.1, 60.0, 42.2, 41.8, 38.8, 35.1, 31.9, 31.2, 25.3, 20.5. MS m/z 260.5 (M+H^{+}).

4.2.3.8. 4-(2-fluorobenzyl)-1-oxa-9-azaspiro[5.5]undecane-9 trifluoroacetate (3o)

Yield 1.02 g (80%). Hygroscopic solid. ^{1}H NMR (300 MHz, DMSO-d_6) δ 8.47 (s, 1H), 8.25 (s, 1H), 7.29 – 7.22 (m, 2H), 7.17 – 7.10 (m, 2H), 3.69 – 3.61 (m, 1H), 3.48 – 3.39 (m, 1H), 3.08 – 2.98 (m, 3H), 2.87 – 2.74 (m, 1H), 2.54 – 2.51 (m, 2H), 2.38– 2.27 (m, 1H), 1.98 – 1.87 (m, 1H), 1.67 – 1.27 (m, 5H), 1.18 – 1.02 (m, 2H). ^{13}C NMR (75 MHz, DMSO-d_6) δ 160.6 (d, J = 242.7 Hz), 131.7 (d, J = 4.8 Hz), 128.1 (d, J = 8.1 Hz), 126.2 (d, J = 16.1 Hz), 124.2 (d, J = 3.5 Hz), 115.1 (d, J = 22.3 Hz), 68.1, 60.0, 41.8, 35.5, 35.3, 31.8, 30.4, 25.5. MS m/z 263.9 (M+H^{+}).

4.2.4. General procedure for the preparation of compounds 3p-r.

Isobutyl chloroformate (0.44 g, 3.19 mmol) was added dropwise under argon to a -30 ºC solution of **11** (1g, 3.19 mmol) and *N*-methylmorpholine (0.39 g, 3.83 mmol) in THF (40 mL). After a brief (30 min) stirring, a solution of the respective amidoxime (3.83 mmol) in THF (10 mL) was added dropwise. The reaction mixture was allowed to reach r. t., stirred at that temperature for 12 h, filtered and concentrated *in vacuo*. The residue was dissolved in toluene (50 mL), TBAF (0.1 g) was added and the mixture was heated at reflux for 5 h with azeotropic removal of water using a Dean-Stark trap. The toluene solution was washed with water, 1% aqueous citric acid, 5% sat. aqueous NaHCO$_3$, brine, dried over anhydrous Na$_2$SO$_4$, filtered and concentrated to dryness *in vacuo*. The residue was fractionated on silica gel using chloroform as eluent. The fractions containing the 1,2,4-oxadiazole product (according to LC MS analysis) were pooled and concentrated *in vacuo*. The residue was dissolved in 1,4-dioxane (15 mL) and treated with 4M HCl in 1,4-dioxane (1 mL). After stirring at r. t. for 6 h, the reaction mixture was concentrated to dryness *in vacuo* and the residue was crystallized from isopropyl alcohol to provide analytically pure title compound.

4.2.4.1. 4-[(3-Pyridin-3-yl-1,2,4-oxadiazol-5-yl)methyl]-1-oxa-9-azaspiro[5.5]undecane dihydrochloride (3p)

Yield 350 mg (63%). Hygroscopic solid. ^{1}H NMR (300 MHz, DMSO-d_6) δ 10.31 (s, 2H), 9.27 (s, 1H), 8.93 (d, J = 5.09 Hz, 1H), 8.66 (d, J = 7.70 Hz, 1H), 7.89 (dd, J = 7.73, 5.37 Hz, 1H), 7.28 – 7.09 (m, 1H), 3.69 (dd, J = 11.89, 4.41 Hz, 1H), 3.53 (t, J = 11.57 Hz, 1H), 3.07 – 2.73 (m, 6H), 2.42 – 2.26 (m, 2H), 1.88 – 1.51 (m, 5H), 1.35 – 1.11 (m, 2H). ^{13}C NMR (75 MHz, DMSO-d_6) δ 179.7, 165.0, 148.7, 144.4, 138.4, 126.0, 123.9, 68.3, 59.7, 41.0, 38.8, 35.0, 32.5, 31.4, 28.4. MS m/z 315.4 (M+H^{+}).

4.2.4.2. 4-[(3-Cyclopropyl-1,2,4-oxadiazol-5-yl)methyl]-1-oxa-9-azaspiro[5.5]undecane hydrochloride (3q)

Yield 350 mg (59%). White crystalline solid, m. p. = 179 – 187 ºC. ^{1}H NMR (300 MHz, DMSO-d_6) δ 9.17 (s, 2H), 3.71 – 3.62 (m, 1H), 3.54 – 3.45 (m, 1H), 3.08 – 2.95 (m, 3H), 2.88 – 2.73 (m, 3H), 2.38 – 2.32 (m, 1H), 2,21– 2,03 (m, 2H), 1.82 – 1.45 (m, 5H), 1.24 – 1.01 (m, 4H), 0,88 – 0.83 (m, 2H). ^{13}C NMR (75 MHz, DMSO-d_6) δ 178.3, 172.1, 68.7, 60.2, 41.5, 35.5, 32.9, 31.8, 28.7, 25.7, 7.8, 6.7. MS m/z 278.5 (M+H^{+}).

4.2.4.3. 4-[(3-(2-methoxyethyl)-1,2,4-oxadiazol-5-yl)methyl]-1-oxa-9-azaspiro[5.5]undecane hydrochloride (3r)

Yield 330 mg (55%). White crystalline solid, m. p. = 132 – 135 ºC. ^{1}H NMR (300 MHz, DMSO-d_6) δ 9.18 (s, 2H), 3.70 – 3.63 (m, 3H), 3.55 – 3.47 (m, 1H), 3.22 (s, 3H), 3.05 – 2.87 (m, 6H), 2.83 (d, J = 6.91 Hz, 2H), 2.39 - 2.32 (m, 1H), 2.26 – 2.15 (m, 1H), 1.82 – 1.72 (m, 1H), 1.58 – 1.53 (m, 4H), 1.23 – 1.07 (m, 2H). ^{13}C NMR (75 MHz, DMSO-d_6) δ 177.9, 168.0, 68.4, 68.2, 59.7, 57.8, 41.0, 38.8, 35.0, 32.3, 31.3, 28.2, 26.0, 25.2. MS m/z 296.3 (M+H^{+}).

4.2.5. General procedure for the preparation of compounds 4a-s.

A solution of the respective spirocyclic piperidine salt **3a-r** or **12** (0.46 mmol) in CH_2Cl_2 (5 mL) was treated with trimethylamine (n x 0.46 mmol, where n = number of salt parts per molecule) followed by a solution of **2** (0.44 mmol) in CH_2Cl_2 (5 mL). After a brief stirring (15 min), sodium triacetoxyboohydride (STAB, 1.32 mmol) was added and the stirring continued for 12 h at r. t. The reaction was poured into 10% aqueous $NaHCO_3$ (20 mL). Organic phase was separated and the aqueous phase was extracted with CH_2Cl_2 (2 x 10 mL). The combined organic extracts were washed with brine, dried over anhydrous Na_2SO_4, filtered and concentrated *in vacuo*. The residue was fractionated on silica gel using 0→1% MeOH in CH_2Cl_2. The fractions containing the reductive amination product (according to LC MS analysis) were pooled and concentrated *in vacuo*. The residue was dissolved in CH_2Cl_2 (3 mL) and treated with TFA (1 mL). The mixture was stirred at r. t. for 18 h and concentrated *in vacuo*. 2M HCl in ether (3 mL) was added to the residue and the later

was triturated (with occasional sonication) until a crystalline hydrochloride salt formed. The latter was separated by filtration, washed with ether and dried *in vacuo* to provide analytically pure compounds **4a-s**.

4.2.5.1. 3-[4-({4-[(4-Methyl-1-oxa-9-azaspiro[5.5]undec-9-yl)methyl]benzyl}oxy)phenyl] propanoic acid hydrochloride (4a).

Yield 26.3 mg (0.06 mmol, 13.6 %). White crystalline solid, m. p. = 183 – 187 ℃. ^{1}H NMR (300 MHz, DMSO-d_6) δ 11.49 (s, 1H), 7.69 (d, J = 7.8 Hz, 2H), 7.47 (d, J = 7.7 Hz, 2H), 7.12 (d, J = 8.2 Hz, 2H), 6.92 (d, J = 8.3 Hz, 2H), 5.08 (s, 2H), 4.40 – 4.22 (m, 2H), 3.53 – 3.43 (m, 4H), 3.11 – 3.01 (m, 2H), 2.77 (t, J = 7.4 Hz, 2H), 2.57 (t, J = 7.4 Hz, 2H), 2.46 – 2.37 (m, 1H), 2.13 – 1.88 (m, 2H), 1.81 – 1.68 (m, 2H), 1.59 – 1.34 (m, 2H), 129 1.11 – 0.81 (m, 5H). ^{13}C NMR (75 MHz, DMSO-d_6) δ 172.7, 156.6, 138.4, 132.7, 131.6, 129.4, 129.2, 127.7, 114.6, 68.7, 67.9, 60.2, 58.2, 51.2, 46.9, 43.9, 35.1, 34.0, 29.4, 25.4, 24.4, 22.2. HRMS (ESI) *m/z* calcd for $C_{27}H_{35}NO_4$ [M+H$^+$] 438.2644, found 438.2598.

4.2.5.2. 3-[4-({4-[(4-Ethoxy-1-oxa-9-azaspiro[5.5]undec-9-yl)methyl]benzyl}oxy)phenyl]propanoic acid hydrochloride (4b).

Yield 73 mg (0.16 mmol, 35.5 %). White crystalline solid, m. p. = 182 – 186 ℃. ^{1}H NMR (300 MHz, DMSO-d_6) δ 11.48 (s, 1H), 7.69 (d, J = 7.9 Hz, 2H), 7.47 (d, J = 7.8 Hz, 2H), 7.13 (d, J = 8.4 Hz, 2H), 6.91 (d, J = 8.4 Hz, 2H), 5.08 (s, 2H), 4.41 – 4.20 (m, 2H), 3.75 – 3.56 (m, 2H), 3.52 - 3.47 (m, 1H), 3.42 (dd, J = 14.0, 7.0 Hz, 2H), 3.10 – 2.83 (m, 4H), 2.74 (t, J = 7.4 Hz, 2H), 2.47 (t, J = 7.7 Hz, 2H), 2.19 - 1.62 (m, 6H), 1.38 – 1.18 (m, 2H), 1.07 (t, J = 7.0 Hz, 3H). ^{13}C NMR (75 MHz, DMSO-d_6) δ 173.7, 156.5, 138.4, 133.1, 131.6, 129.3, 129.2, 127.7, 114.5, 70.2, 68.7, 68.6, 62.1, 58.3, 58.2, 46.8, 46.6, 41.0, 35.6, 33.5, 31.9, 29.5, 28.0, 15.5. HRMS (ESI) *m/z* calcd for $C_{28}H_{37}NO_5$ [M+H$^+$] 468.2750, found 468.2754.

4.2.5.3. 3-{4-[(4-{[4-(Cyclopropylmethoxy)-1-oxa-9-azaspiro[5.5]undec-9-yl]methyl}benzyl)oxy]phenyl}propanoic acid hydrochloride (4c)

Yield 30 mg (0.06 mmol, 13.9 %). Hygroscopic solid. ^{1}H NMR (300 MHz, DMSO-d_6) δ 11.47 (s, 1H), 7.69 (d, J = 8.0 Hz, 2H), 7.47 (d, J = 7.9 Hz, 2H), 7.12 (d, J = 8.4 Hz, 2H), 6.91 (d, J = 8.4 Hz, 2H), 5.08 (s, 2H), 4.40 – 4.20 (m, 2H), 3.73 – 3.58 (m, 2H), 3.53 – 3.44 (m, 1H), 3.25 (dd, J = 14.7, 6.6 Hz, 2H), 3.11 – 2.84 (m, 4H), 2.76 (q, J = 7.9 Hz, 2H), 2.57 (t, J = 7.5 Hz, 2H), 2.19 – 1.54 (m, 6H), 1.39 – 1.16 (m, 2H), 1.01 – 0.87 (m, 1H), 0.42 (d, J = 7.6 Hz, 2H), 0.13 (d, J = 4.7 Hz, 2H). ^{13}C NMR (75 MHz, DMSO-d_6) δ 173.7, 156.6, 138.4, 133.1, 132.7, 131.6, 129.3, 129.2, 127.7,

114.6, 71.4, 70.1, 68.7, 58.3, 58.2, 51.2, 46.8, 46.6, 35.6, 35.1, 33.5, 31.9, 29.4, 28.1, 10.8, 2.9, 2.8. HRMS (ESI) m/z calcd for $C_{30}H_{39}NO_5$ [M+H$^+$] 494.2906, found 494.2901.

4.2.5.3. 3-(4-{[4-({4-[(3-Fluorobenzyl)oxy]-1-oxa-9-azaspiro[5.5]undec-9-yl}methyl)benzyl]oxy}phenyl)propanoic acid hydrochloride (4d)

Yield 90 mg (0.165 mmol, 37.5 %). White crystalline solid, m. p. = 187 – 190 ºC. ^{1}H NMR (300 MHz, DMSO-d_6) δ 10.87 (s, 1H), 7.63 (d, J = 8.05 Hz, 2H), 7.49 (d, J = 7.96 Hz, 2H), 7.40 – 7.33 (m, 1H), 7.16 – 7.05 (m, 5H), 6.92 (d, J = 8.60 Hz, 2H), 5.09 (s, 2H), 4.56 – 4.51 (m, 2H), 4.39 – 4.25 (m, 2H), 3.76 – 3.69 (m, 1H), 3.58 – 3.35 (m, 2H), 3.16 – 2.83 (m, 4H), 2.74 (t, J = 7.59 Hz, 2H), 2.48 (t, J = 7.59 Hz, 2H), 2.17 – 2.10 (m, 1H), 1.95 – 1.75 (m, 5H), 1.49 – 1.31 (m, 2H). ^{13}C NMR (75 MHz, DMSO-d_6) δ 173.8, 162.1 (d, J = 243.2 Hz), 165.5, 142.0 (d, J = 7.1 Hz), 138.5, 133.1, 131.59, 130.2 (d, J = 8.3 Hz), 129.3, 129.2, 127.8, 123.0 (d, J = 2.7 Hz), 114.6, 113.9 (d, J = 20.9 Hz), 113.7 (d, J = 21.4 Hz), 70.6, 68.7, 68.6, 68.0, 58.4, 58.3, 46.9, 46.8, 35.5, 33.5, 31.6, 30.7, 29.5, 28.3. HRMS (ESI) m/z calcd for $C_{33}H_{38}FNO_5$ [M+H$^+$] 548.2812, found 548.2806.

4.2.5.4. 3-[4-({4-[(4-{[4-(Trifluoromethyl)benzyl]oxy}-1-oxa-9-azaspiro[5.5]undec-9-yl)methyl]benzyl}oxy)phenyl]propanoic acid hydrochloride (4e)

Yield 59 mg (0.09 mmol, 21.5 %). White crystalline solid, m. p. = 128 – 131 ºC. ^{1}H NMR (300 MHz, DMSO-d_6) δ 10.95 (s, 1H), 7.71– 7.62 (m, 4H), 7.55– 7.47 (m, 4H), 7.13 (d, J = 8.56 Hz, 2H), 6.92 (d, J = 8.65 Hz, 2H), 5.08 (s, 2H) , 4.65– 4.60 (m, 2H), 4.37– 4.25 (m, 2H), 3.78 – 3.72 (m, 2H), 3.54 – 3.46 (m, 1H), 3.15 – 2.86 (m, 4H), 2.74 (t, J = 7.55 Hz, 2H), 2.48 (t, J = 7.55 Hz, 2H), 2.19 – 2.11 (m, 1H), 2.01 – 1.78 (m, 5H), 1.49 – 1.31 (m, 2H). ^{13}C NMR (75 MHz, DMSO-d_6) δ 173.8, 156.5, 143.0, 138.5, 133.1, 131.6, 129.3, 129.2, 127.9 (q, J = 13.8 Hz), 127.8, 127.6, 125.1 (q, J = 3.8 Hz), 124.3 (q, J = 271.9 Hz), 114.5, 70.8, 68.7, 68.6, 68.0, 58.3, 58.3, 46.9, 46.8, 40.8, 35.5, 33.5, 31.6, 29.5, 28.3 HRMS (ESI) m/z calcd for $C_{34}H_{38}F_3NO_5$ [M+H$^+$] 598.2780, found 598.2798.

4.2.5.5. 3-{4-[(4-{[4-(Benzyloxy)-1-oxa-9-azaspiro[5.5]undec-9-yl]methyl}benzyl)oxy]phenyl}propanoic acid hydrochloride (4f)

Yield 13 mg (0.026 mmol, 5.9 %). Hygroscopic solid. ^{1}H NMR (300 MHz, DMSO-d_6) δ 11.47 (s, 1H), 7.68 (d, J = 7.8 Hz, 2H), 7.47 (d, J = 7.7 Hz, 2H), 7.35 – 7.24 (m, 5H), 7.13 (d, J = 8.2 Hz, 2H), 6.91 (d, J = 8.2 Hz, 2H), 5.08 (s, 2H), 4.51 (d, J = 14.0 Hz, 2H), 4.41 – 4.21 (m, 2H), 3.75 – 3.65 (m, 2H), 3.50 – 3.45 (m, 1H), 3.10 – 2.82 (m, 4H), 2.74 (t, J = 7.4 Hz, 2H), 2.46 (t, J = 7.3 Hz, 2H), 2.17 – 1.71 (m, 6H), 1.36 (dd, J = 23.6, 13.6 Hz, 2H). ^{13}C NMR (75 MHz, DMSO-d_6) δ 173.7, 156.5, 138.8, 138.4, 133.1, 131.6, 129.2, 128.2, 128.1, 127.7, 127.2, 114.5, 72.1, 70.4, 68.8, 68.6,

60.1, 58.2, 46.8, 46.6, 40.8, 35.5, 33.3, 31.6, 29.4, 28.2. HRMS (ESI) *m/z* calcd for $C_{33}H_{39}NO_5$ [M+H$^+$] 530.2906, found 530.2916.

4.2.5.6. 3-(4-{[4-({4-[(4-Fluorobenzyl)oxy]-1-oxa-9-azaspiro[5.5]undec-9-yl}methyl)benzyl]oxy}phenyl)propanoic acid hydrochloride (4g)

Yield 20 mg (0.038 mmol, 8.6 %). White crystalline solid, m. p. = 71 – 78 ℃. ^{1}H NMR (300 MHz, DMSO-*d$_6$*) δ 11.49 (s, 1H), 7.71 – 7.67 (m, 2H), 7.49 – 7.45 (m, 2H), 7.37 – 7.32 (m, 2H), 7.17 – 7.11 (m, 4H), 6.91 (d, *J* = 8.14 Hz, 2H), 5.07 (s, 2H), 4.52 – 4.47 (m, 2H), 4.39– 4.24 (m, 2H), 3.78 – 3.64 (m, 2H), 3.52 – 3.42 (m, 1H), 3.11 – 2.82 (m, 4H), 2.73 (t, *J* = 7.55 Hz, 2H), 2.48 (t, *J* = 7.55 Hz, 2H), 2.17 – 1.71 (m, 6H), 1.44 – 1.22 (m, 2H). ^{13}C NMR (75 MHz, DMSO-*d$_6$*) δ 173.7, 161.3 (d, *J* = 242.7 Hz), 156.5, 138.4, 135.0 (d, *J* = 2.7 Hz), 133.1, 131.6, 129.3, 129.3 (d, *J* = 8.1 Hz), 127.7, 114.9 (d, *J* = 21.2 Hz), 114.5, 70.4, 70.4, 68.7, 68.6, 68.0, 58.2, 46.8, 46.6, 40.8, 35.5, 33.4, 31.6, 29.4, 28.2. HRMS (ESI) *m/z* calcd for $C_{33}H_{38}FNO_5$ [M+H$^+$] 548.2812, found 548.2782.

4.2.5.7. 3-[4-({4-[(4-Methyl-1-oxa-9-azaspiro[5.5]undec-9-yl)methyl]benzyl}oxy)phenyl]propanoic acid hydrochloride (4h)

Yield 26 mg (0.06 mmol, 13.6 %). White crystalline solid, m. p. = 183 – 187 ℃. ^{1}H NMR (300 MHz, DMSO-*d$_6$*) δ 11.49 (s, 1H), 7.69 (d, *J* = 7.8 Hz, 2H), 7.47 (d, *J* = 7.7 Hz, 2H), 7.12 (d, *J* = 8.2 Hz, 2H), 6.92 (d, *J* = 8.3 Hz, 2H), 5.08 (s, 2H), 4.40 – 4.22 (m, 2H), 3.53 – 3.43 (m, 4H), 3.11 – 3.01 (m, 2H), 2.77 (t, *J* = 7.4 Hz, 2H), 2.57 (t, *J* = 7.4 Hz, 2H), 2.46 – 2.37 (m, 1H), 2.13 – 1.88 (m, 2H), 1.81 – 1.68 (m, 2H), 1.59 – 1.34 (m, 2H), 129 1.11 – 0.81 (m, 5H). ^{13}C NMR (75 MHz, DMSO-*d$_6$*) δ 172.6, 156.6, 138.3, 132.7, 131.5, 129.3, 129.2, 127.7, 114.6, 68.6, 67.8, 60.1, 58.2, 51.2, 46.8, 43.9, 35.1, 34.0, 29.3, 25.4, 24.4, 22.2. HRMS (ESI) *m/z* calcd for $C_{27}H_{35}NO_4$ [M+H$^+$] 438.2644, found 438.2598.

4.2.5.7. 3-(4-{[4-({4-[4-(Trifluoromethyl)benzyl]-1-oxa-9-azaspiro[5.5]undec-9-yl}methyl)benzyl]oxy}phenyl)propanoic acid hydrochloride (4i)

Yield 78 mg (0.135 mmol, 30.7 %). White crystalline solid, m. p. = 176 – 185 ℃. ^{1}H NMR (300 MHz, DMSO-*d$_6$*) δ 11.53 (s, 1H), 7.65 (dd, *J* = 7.96, 18.53 Hz, 4H), 7.45 (d, *J* = 8.05 Hz, 2H), 7.39 (d, *J* = 8.01 Hz, 2H), 7.13 (d, *J* = 8.51 Hz, 2H), 6.92 (d, *J* = 8.51 Hz, 2H), 5.08 (s, 2H), 4.38 – 4.22 (m, 2H), 3.71 – 3.58 (m, 1H), 3.51 – 3.39 (m, 1H), 3.08 – 2.80 (m, 4H), 2.75 (t, *J* = 7.56 Hz, 2H), 2.60 – 2.52 (m, 2H), 2.48 (t, *J* = 7.56 Hz, 2H), 2,44 – 2.39 (m, 1H), 2.10 – 0.99 (m, 8H). ^{13}C NMR (75 MHz, DMSO-*d$_6$*) δ 173.7, 156.5, 144.7 (d, J = 1.0 Hz), 138.4, 133.1, 131.6, 129.8, 129.2, 127.8, 126.7 (q, *J* = 31.66 Hz), 125.0 (q, *J* = 3.63 Hz), 122.7, 114.6, 68.7, 68.0, 60.0, 58.2, 46.8, 46.7,

42.2, 41.7, 35.6, 35.3, 31.7, 31.3, 29.5, 25.4. HRMS (ESI) *m/z* calcd for $C_{34}H_{38}F_3NO_4$ [M+H$^+$] 582.2831, found 582.2826.

4.2.5.8. 3-{4-[(4-{[4-(3-Fluorobenzyl)-1-oxa-9-azaspiro[5.5]undec-9-yl]methyl}benzyl)oxy]phenyl}propanoic acid hydrochloride (4j)

Yield 29 mg (0.054 mmol, 12.3 %). White crystalline solid, m. p. = 186 – 189 ºC. ^{1}H NMR (300 MHz, DMSO-*d$_6$*) δ 11.55 (s, 1H), 7.69 (d, *J* = 7.60 Hz, 2H), 7.46 (d, *J* = 7.68 Hz, 2H), 7.35 – 7.25 (m, 1H), 7.13 (d, *J* = 8.19 Hz, 2H), 7.03 – 6.90 (m, 5H), 5.08 (s, 2H), 4.38 – 4.22 (m, 2H), 3.70 – 3.60 (m, 1H), 3.50 – 3.38 (m, 1H), 3.09 – 2.84 (m, 4H), 2.77 (t, *J* = 7.55 Hz, 2H), 2.57 (t, *J* = 7.55 Hz, 2H), 2.48 – 2.44 (m, 2H), 2,43 – 2.39 (m, 1H), 2.09 – 1.29 (m, 6H), 1.18 – 0.99 (m, 2H). ^{13}C NMR (75 MHz, DMSO-*d$_6$*) δ 172.6, 162.1 (d, *J* = 243.0 Hz), 156.6, 142.7 (d, *J* = 7.2 Hz), 138.3, 132.7, 131.5, 129.9 (d, *J* = 11.0 Hz), 129.3, 129.2, 127.7, 125.1, 115.7, 115.4, 114.6, 112.8, 112.5, 68.6, 67.9, 60.1, 59.9, 58.1, 51.2, 46.8, 46.7, 42.1, 41.7, 35.1, 31.8, 31.2, 29.3, 25.4. HRMS (ESI) *m/z* calcd for $C_{33}H_{38}FNO_4$ [M+H$^+$] 532.2863, found 532.2858.

4.2.5.9. 3-{4-[(4-{[4-(4-Fluorobenzyl)-1-oxa-9-azaspiro[5.5]undec-9-yl]methyl}benzyl)oxy]phenyl}propanoic acid hydrochloride (4k)

Yield 28 mg (0.052 mmol, 11.8 %). White crystalline solid, m. p. = 200 – 203 ºC. ^{1}H NMR (300 MHz, DMSO-*d$_6$*) δ 11.51 (s, 1H), 7.68 (d, *J* = 7.73 Hz, 2H), 7.47 (d, *J* = 7.77 Hz, 2H), 7.29 – 7.04 (m, 6H), 6.91 (d, *J* = 8.37 Hz, 2H), 5.08 (s, 2H), 4.38 – 4.21 (m, 2H), 3.72 – 3.57 (m, 1H), 3.52 – 3.39 (m, 1H), 3.09 – 2.80 (m, 4H), 2.75 (t, *J* = 7.46 Hz, 2H), 2.49 (t, *J* = 7.50 Hz, 2H), 2.48 (d, *J* = 6.45 Hz, 1H), 2.42 – 2.36 (m, 1H), 2.09 – 1.80 (m, 2H), 1.73 – 1.30 (m, 4H), 1.16 – 0.96 (m, 2H). ^{13}C NMR (75 MHz, DMSO-*d$_6$*) δ 173.6, 160.6 (d, *J* = 241.1 Hz), 156.5, 138.4, 135.6 (d, *J* = 3.1 Hz), 133.1, 131.4, 130.6 (d, *J* = 7.7 Hz), 129.2, 129.1, 127.6, 114.7 (d, *J* = 20.9 Hz), 114.5, 68.6, 67.8, 59.9, 58.3, 46.9, 46.8, 41.6, 35.4, 31.7, 31.4, 29.4, 25.5. HRMS (ESI) *m/z* calcd for $C_{33}H_{38}FNO_4$ [M+H$^+$] 532.2863, found 532.2858.

4.2.5.10. 3-[4-({4-[(4-Benzyl-1-oxa-9-azaspiro[5.5]undec-9-yl)methyl]benzyl}oxy)phenyl]propanoic acid hydrochloride (4l)

Yield 68 mg (0.133 mmol, 38 %). White crystalline solid, m. p. = 283 – 188 ºC. ^{1}H NMR (300 MHz, DMSO-*d$_6$*) δ 10.97 (s, 1H), 7.64 (d, *J* = 7.8 Hz, 2H), 7.48 (d, *J* = 7.8 Hz, 2H), 7.27 (t, *J* = 7.1 Hz, 2H), 7.20 – 7.11 (m, 5H), 6.91 (d, *J* = 8.4 Hz, 2H), 5.08 (s, 2H), 4.39 – 4.22 (m, 2H), 3.62 (dd, *J* = 11.8, 4.8 Hz, 1H), 3.42 (t, *J* = 11.4 Hz, 1H), 3.13 – 2.80 (m, 4H), 2.74 (t, *J* = 7.6 Hz, 2H), 2.46 (t, *J* = 7.4 Hz, 2H), 2.44 – 2.36 (m, 2H), 2.05 – 1.79 (m, 2H), 1.65 – 1.29 (m, 4H), 1.20 – 0.94 (m, 2H). ^{13}C NMR (75 MHz, DMSO-*d$_6$*) δ 173.9, 156.6, 139.7, 138.5, 133.1, 131.6, 129.3, 129.3,

129.0, 128.2, 127.8, 125.9, 114.6, 68.6, 67.9, 60.1, 58.3, 47.0, 46.9, 42.7, 41.8, 35.6, 31.9, 31.5, 30.7, 29.5, 25.6. HRMS (ESI) *m/z* calcd for $C_{33}H_{39}NO_4$ [M+H$^+$] 514.2957, found 514.2966.

4.2.5.11. 3-{4-[(4-{[4-(4-Methoxybenzyl)-1-oxa-9-azaspiro[5.5]undec-9-yl]methyl}benzyl)oxy]phenyl}propanoic acid hydrochloride (4m)

Yield 98 mg (0.181 mmol, 41 %). White crystalline solid, m. p. = 161 – 165 ºC. ^{1}H NMR (300 MHz, DMSO-*d$_6$*) δ 11.06 (s, 1H), 7.65 (d, *J* = 7.9 Hz, 2H), 7.48 (d, *J* = 7.9 Hz, 2H), 7.13 (d, *J* = 8.4 Hz, 2H), 7.05 (d, *J* = 8.4 Hz, 2H), 6.91 (d, *J* = 8.5 Hz, 2H), 6.82 (d, *J* = 8.4 Hz, 2H), 5.08 (s, 2H), 4.40 – 4.22 (m, 2H), 3.70 (s, 3H), 3.62 (dd, *J* = 11.1, 3.5 Hz, 1H), 3.41 (t, *J* = 11.6 Hz, 1H), 3.13 – 2.79 (m, 4H), 2.74 (t, *J* = 7.5 Hz, 2H), 2.48 – 2.29 (m, 5H), 2.03 – 1.75 (m, 2H), 1.62 – 1.28 (m, 4H), 1.12 – 0.94 (m, 2H). ^{13}C NMR (75 MHz, DMSO-*d$_6$*) δ 174.2, 157.9, 157.0, 138.9, 133.5, 132.0, 131.8, 130.3, 129.79, 129.7, 128.2, 115.0, 114.0, 69.1, 68.3, 60.5, 58.7, 55.3, 47.4, 47.3, 42.2, 36.0, 35.9, 32.4, 32.1, 29.9, 26.0. HRMS (ESI) *m/z* calcd for $C_{34}H_{41}NO_5$ [M+H$^+$] 544.3063, found 544.3057.

4.2.5.12. 3-{4-[(4-{[4-(4-Methylbenzyl)-1-oxa-9-azaspiro[5.5]undec-9-yl]methyl}benzyl)oxy]phenyl}propanoic acid hydrochloride (4n)

Yield 120 mg (0.227 mmol, 51 %). White crystalline solid, m. p. = 148 – 151 ºC. ^{1}H NMR (300 MHz, DMSO-*d$_6$*) δ 11.02 (s, 1H), 7.64 (d, *J* = 8.0 Hz, 1H), 7.48 (d, *J* = 7.9 Hz, 1H), 7.13 (d, *J* = 8.5 Hz, 1H), 7.04 (dd, *J* = 14.9, 7.9 Hz, 2H), 6.91 (d, *J* = 8.5 Hz, 1H), 5.08 (s, 1H), 4.40 – 4.21 (m, 1H), 3.62 (dd, *J* = 11.4, 4.0 Hz, 1H), 3.42 (t, *J* = 11.6 Hz, 1H), 3.11 – 2.79 (m, 2H), 2.74 (t, *J* = 7.5 Hz, 1H), 2.49 – 2.36 (m, 3H), 2.25 (s, 2H), 2.02 – 1.78 (m, 1H), 1.63 – 1.27 (m, 2H), 1.17 – 0.96 (m, 1H). ^{13}C NMR (75 MHz, DMSO-*d$_6$*) δ 173.8, 156.5, 138.5, 136.5, 134.8, 133.1, 131.6, 129.3, 129.2, 128.9, 128.8, 127.8, 114.6, 68.6, 67.9, 60.1, 58.3, 47.0, 46.9, 42.3, 41.8, 35.5, 32.0, 31.5, 30.7, 29.5, 25.5, 20.6. HRMS (ESI) *m/z* calcd for $C_{34}H_{41}NO_4$ [M+H$^+$] 528.3114, found 528.3120.

4.2.5.13. 3-{4-[(4-{[4-(2-Fluorobenzyl)-1-oxa-9-azaspiro[5.5]undec-9-yl]methyl}benzyl)oxy]phenyl}propanoic acid hydrochloride (4o)

Yield 16 mg (0.030 mmol, 6.8 %). Hygroscopic solid. ^{1}H NMR (300 MHz, DMSO-*d$_6$*) δ 11.46 (s, 1H), 7.69 – 7.65 (m, 2H), 7.48 – 7.45 (m, 2H), 7.28 – 7.21 (m, 2H), 7.15 – 7.09 (m, 4H), 6.91 (d, *J* = 8.14 Hz, 2H), 5.07 (s, 2H), 4.38 – 4.22 (m, 2H), 3.72 – 3.58 (m, 1H), 3.50 – 3.37 (m, 1H), 3.07 – 2.81 (m, 4H), 2.74 (t, *J* = 7.55 Hz, 2H), 2.56 – 2.51 (m, 2H), 2.48 (t, *J* = 7.55 Hz, 2H), 2.44 – 2.37 (m, 1H), 2.04 – 1.84 (m, 2H), 1.69 – 1.29 (m, 4H), 1.20 – 1.02 (m, 2H). ^{13}C NMR (75 MHz, DMSO-*d$_6$*) δ 173.6, 160.5 (d, *J* = 242.7 Hz), 156.5, 138.3, 133.0, 131.6 (d, *J* = 4.6 Hz), 131.5, 129.3, 129.1, 128.1 (d, *J* = 8.1 Hz), 127.6, 126.2 (d, *J* = 15.9 Hz), 124.1 (d, *J* = 3.8 Hz), 115.0 (d, *J*

= 21.9 Hz), 114.5, 68.6, 67.8, 59.9, 58.1, 46.8, 46.7, 43.5, 41.6, 35.5, 35.3, 31.8, 29.4, 25.3. HRMS (ESI) *m/z* calcd for $C_{33}H_{38}FNO_4$ [M+H$^+$] 532.2863, found 532.2885.

4.2.5.14. 3-(4-{[4-({4-[(3-Pyridin-3-yl-1,2,4-oxadiazol-5-yl)methyl]-1-oxa-9-azaspiro[5.5]undec-9-yl}methyl)benzyl]oxy}phenyl)propanoic acid dihydrochloride (4p)

Yield 61 mg (0.105 mmol, 24 %). White crystalline solid, m. p. = 232 – 235 ºC. ^{1}H NMR (300 MHz, DMSO-d_6) δ 11.50 (s, 1H), 9.26 – 9.19 (m, 1H), 8.90 (d, *J* = 4.1 Hz, 1H), 8.58 (d, *J* = 7.0 Hz, 1H), 7.83 (dd, *J* = 7.8, 5.2 Hz, 1H), 7.69 (d, *J* = 7.9 Hz, 2H), 7.47 (d, *J* = 7.9 Hz, 2H), 7.13 (d, *J* = 8.5 Hz, 2H), 6.91 (d, *J* = 8.5 Hz, 2H), 5.07 (s, 2H), 4.44 – 4.20 (m, 2H), 3.72 – 3.61 (m, 1H), 3.58 – 3.45 (m, 1H), 3.12 – 2.81 (m, 6H), 2.73 (t, *J* = 7.5 Hz, 2H), 2.46 (t, *J* = 7.4 Hz, 2H), 2.33 – 2.21 (m, 1H), 2.13 – 1.46 (m, 6H), 1.35 – 1.14 (m, 2H). ^{13}C NMR (75 MHz, DMSO-d_6) δ 179.6, 173.8, 165.3, 156.6, 149.6, 145.3, 138.4, 137.5, 133.1, 131.6, 129.4, 129.2, 127.7, 125.6, 123.6, 114.6, 68.7, 68.0, 59.8, 58.3, 46.8, 41.2, 35.6, 35.3, 32.5, 31.4, 30.7, 29.5, 28.6. HRMS (ESI) *m/z* calcd for $C_{34}H_{38}N_4O_5$ [M+H$^+$] 583.2920, found 583.2924.

4.2.5.15. 3-(4-{[4-({4-[(3-Cyclopropyl-1,2,4-oxadiazol-5-yl)methyl]-1-oxa-9-azaspiro[5.5]undec-9-yl}methyl)benzyl]oxy}phenyl)propanoic acid hydrochloride (4q)

Yield 67 mg (0.123 mmol, 28 %). White crystalline solid, m. p. = 179 – 184 ºC. ^{1}H NMR (300 MHz, DMSO-d_6) δ 11.45 (s, 1H), 7.68 (d, *J* = 6.40 Hz, 2H), 7.47 (d, *J* = 6.08 Hz, 2H), 7.12 (d, *J* = 7.41 Hz, 2H), 6.91 (d, *J* = 7.51 Hz, 2H), 5.07 (s, 2H), 4.39 – 4.24 (m, 2H), 3.68 – 3.59 (m, 1H), 3.52 – 3.39 (m, 1H), 3.11 – 2.99 (m, 3H), 2.87 – 2.70 (m, 5H), 2.48 – 2.39 (m, 3H), 2,18– 2,01 (m, 3H), 1.79 – 1.38 (m, 4H), 1.23 – 0.99 (m, 4H), 0,88 – 0.82 (m, 2H). ^{13}C NMR (75 MHz, DMSO-d_6) δ 177.8, 173.6, 171.5, 156.5, 138.3, 133.0, 131.5, 129.3, 129.1, 127.6, 114.5, 68.6, 67.8, 59.7, 58.1, 46.7, 35.5, 32.3, 31.3, 29.4, 28.3, 25.3, 7.3, 6.2. HRMS (ESI) *m/z* calcd for $C_{32}H_{39}N_3O_5$ [M+H$^+$] 546.2968, found 546.2962.

4.2.5.16. 3-[4-({4-[(4-{[3-(2-Methoxyethyl)-1,2,4-oxadiazol-5-yl]methyl}-1-oxa-9-azaspiro[5.5]undec-9-yl)methyl]benzyl}oxy)phenyl]propanoic acid hydrochloride (4r)

Yield 98 mg (0.174 mmol, 40 %). White crystalline solid, m. p. = 166 – 176 ºC. ^{1}H NMR (300 MHz, DMSO-d_6) δ 10.87 (s,1H), 7.56 (AB$_q$, *J* = 8.10, 45.05 Hz, 4H), 7.03 (AB$_q$, *J* = 8.60, 57.86 Hz, 4H), 5.08 (s, 2H), 4.38 – 4.24 (m, 2H), 3.68 – 3.62 (m, 3H), 3.54– 3.45 (m, 1H), 3.21 (s, 3H), 3.09 – 3.03 (m, 3H), 2.92 - 2.81 (m, 5H), 2.74 (t, *J* = 7.64 Hz, 2H), 2.49 – 2.44 (m, 3H), 2.25 – 2.10 (m, 1H), 2.07 – 1.85 (m, 1H), 1.68 – 1.42 (m, 4H), 1.24 – 1.05 (m, 2H). ^{13}C NMR (75 MHz, DMSO-d_6) δ 177.9, 173.6, 168.0, 156.5, 138.5, 133.1, 131.4, 129.2, 129.1, 127.1, 114.5, 68.6, 68.3,

67.8, 59.7, 58.3, 57.8, 46.8, 41.1, 35.4, 35.3, 32.3, 31.3, 29.4, 28.3, 25.9, 25.4. HRMS (ESI) *m/z* calcd for $C_{32}H_{41}N_3O_6$ [M+H$^+$] 564.3074, found 564.3083.

4.2.5.17. 3-(4-{[4-(1-Oxa-9-azaspiro[5.5]undec-9-ylmethyl)benzyl]oxy}phenyl)propanoic acid hydrochloride (4s)

Yield 12 mg (0.029 mmol, 6.6 %). White crystalline solid, m. p. = 194 – 199 ºC. ^{1}H NMR (300 MHz, DMSO-d_6) δ 11.38 (s, 1H), 7.68 (d, *J* = 7.5 Hz, 2H), 7.48 (d, *J* = 7.6 Hz, 2H), 7.13 (d, *J* = 8.1 Hz, 2H), 6.91 (d, *J* = 8.2 Hz, 2H), 5.08 (s, 2H), 4.39 – 4.22 (m, 2H), 3.53 (br s, 2H), 3.1-2.87 (m, 4H), 2.74 (t, *J* = 7.3 Hz, 2H), 2.48 (t, *J* = 7.8 Hz, 2H), 2.03 (d, *J* = 14.2 Hz, 2H), 1.84 (t, *J* = 12.7 Hz, 2H), 1.6-1.3 (m, 6H). ^{13}C NMR (75 MHz, DMSO-d_6) δ 173.7, 156.5, 138.3, 133.0, 131.5, 129.4, 129.2, 127.7, 114.55, 68.6, 67.3, 60.1, 58.2, 46.7, 35.5, 35.1, 30.7, 30.1, 29.4, 25.3, 18.1. HRMS (ESI) *m/z* calcd for $C_{26}H_{33}NO_4$ [M+H$^+$] 424.2488, found 424.2502.

4.3 Molecular modeling

4.3.1. Protein structure source and preparation for docking

The 3D coordinates for FFA1 co-crystalized with TAK-875 were obtained from the Protein Data Bank (PDB ID: 4PHU) and used for subsequent docking procedures.[23] Protein preparation, refinement and docking was performed within Schrödinger's Maestro, version 2016-1.[24] To prepare FFA1 for docking, hydrogens and missing atoms were added, alternate residue positions were defined and the hydrogen bonding network was further optimized by re-orientating hydroxyls, amides and imidazole rings (of histidine residues) using Protein Preparation Wizard.[25]

4.3.2. Docking protocol.

In the crystallized FFA1, four point mutations (Leu42-Ala, Phe88-Ala, Gly103-Ala, Tyr202-Phe) were made to increase expression of the protein and to improve thermal stability. The mutant Ala88, positioned between TM3 and TM4 can be considered an important residue in stabilizing the binding conformations.[26] Therefore, this residue was mutated *in silico* back to Phe with extensive conformational sampling using the MacroModel Conformational Search.[27] To alleviate any strain occurring from this point mutation, a stringent two-step minimization protocol was employed, i.e. hydrogen-only minimization followed by a constrained minimization based on the X-Ray derived B-Factors, implemented with MacroModel.[27] In determining the final position of the benzyl side-chain in **4l** and for selecting an appropriate docking protocol, TAK-875 was re-docked onto FFA1 and compared to the crystal structure orientation, RMSD < 2.5 Å. Furthermore, in determining a correct docking pose an appreciation of the membrane positioning was made using the Orientation

of proteins in membrane (OPM) database and PPM webserver to align and perdict the position of the GPR40 receptor in a membrane.[28] Ligands were created manually in the Schrödinger Maestro 2D sketcher and prepared using LigPrep[29] to produce a low energy conformation. Receptor grid generation and docking was performed using GLIDE[30] with the extra precision (XP) algorithm while enhancing the planarity of conjugated pi groups. The centroid of the grid was defined by the center of mass of TAK-875 as positioned in the crystal structure. In all calculations the OPLS3, all atom force-field was utilized. To allow the comparison of residue positions within the GPCR family, the labels in figure 1 and figure 2 shown the Ballesteros Weinstein indexing system in subscript.[21] Images were rendered using two separate programs: maestro to represent the specific protein-ligand interactions and VMD v1.9.2[31] to visualize the membrane position and surface representations.

4.4 Biological and ADME assays

4.4.1. Determination of agonistic activity of compounds against FFA1 (GPR40), FFA3 (GPR41), FFA2 (GPR43) and FFA4 (GPR120) receptors

CHO cells stably expressing human GPR40 (stable CHO-GPR40 line created at Enamine Ltd.) were seeded (12500 cells/well) into 384-well black-wall, clear-bottom microtiter plates 24 h prior to assay. Cells were loaded for 1 h with fluorescent calcium dye (Fluo-8 Calcium Assay kit, Abcam, ab112129) and tested using fluorometric imaging plate reader (FLIPR Tetra® High Throughput Cellular Screening System, Molecular Devices Corp.). Maximum change in fluorescence over base line was used to determine agonist response. A potent and selective agonist for FFA1 (GPR40) GW9508 (Selleckchem, S8014) was tested with the test compounds as a positive control. Concentration response curve data were fitted using Molecular Devices ScreenWorks® System Control Software (Molecular Devices). For specificity screening for possible GPR41, GPR43 and GPR120agonism, CHO cell lines stably expressing the respective receptors (purchased from The European Collection of Cell Cultures, ECACC) were used.

4.4.2. Determination of aqueous solubility (PBS, pH 7.4)

The test compounds (**4k-n**) and the reference compound (Ondansetron hydrochloride, Sigma-Aldrich, O3639), were assessed for kinetic solubility in phosphate-buffered saline: 138 mM NaCl, 2.7 mM KCl, 10 mM K-phosphate, pH 7.4 with 2% final DMSO. Solubility measurements were done using filter microplate technique with UV-quantification for all compounds. Using a 40 mM stock solution of each compound in 100% DMSO, dilutions were prepared to a theoretical concentration of 800 μM in duplicates in phosphate-buffered saline pH 7.4 with 2% final dimethyl

sulfoxide (DMSO) and then transferred to a 96-well, deep well polypropylene collection plate. In parallel, compound dilutions in 50% methanol/PBS mixes were prepared at concentrations of 0 µM (blank), 200 µM and 400 µM in duplicates to generate calibration curves. The experimental compound dilutions in PBS were further allowed to equilibrate at 25°C on a thermostatic orbital shaker for two hours and then filtered through HTS solubility filter plates (EMD Millipore, MSSLBPC) using a vacuum manifold. The filtrates adjusted for the calibration sample non-aqueous solvent content by 2-fold dilution with methanol, and the calibrating solutions were analyzed using SpectraMax UV-Vis microplate reader (200-550 nm absorbance scan, 5 nm step increment). The concentrations of compounds in PBS filtrate were determined using a dedicated Microsoft Excel calculation script. Proper absorbance wavelengths for calculations were selected for each compound manually based on absorbance maxima (absolute absorbance unit values for the minimum and maximum concentration points within 0 - 3 OD range). Each of the final datasets was additionally visually evaluated by the operator and goodness of fit (R^2) was calculated for each calibration curve. The reference compound was included in every separate solubility experiment to control proper assay performance.

4.4.3. Assessment of metabolic stability in mouse liver microsomes

The metabolic stability of compounds **4k-n** as well as the reference compounds (Imipramine, Propranolol) was determined in liver microsomes at five time points over 40 minutes using HPLC-MS.

Mouse hepatic microsomes were isolated from pooled (50), perfused livers of BALB/c male mice according to the standard protocol.[32] The batch of microsomes was tested for quality control using a commercial comparator preparation (Sigma-Aldrich M9441) and verapamil and propranolol as reference compounds. Microsomal incubations were carried out in 96-well plates in 5 aliquots of 40 µL each (one for each time point). Liver microsomal incubation medium contained potassium phosphate buffer (100 mM, pH 7.4), $MgCl_2$ (3.3 mM), NADPH (3 mM), glucose-6-phosphate (5.3 mM), glucose-6-phosphate dehydrogenase (0.67 units/ml) with 0.42 mg of liver microsomal protein per ml. In addition, control incubations were performed replacing the NADPH-regenerating system with 100 mM phosphate buffer pH 7.4. Test compounds (2 µM, final solvent concentration 1.6 %) were incubated at 37°C under vortexing at 100 rpm. Five time points over 40 minutes had been analyzed. The reactions were stopped by adding 12 volumes of 90% acetonitrile-water to 40 µL incubation aliquots, followed by plasma protein precipitation by centrifuging at 5500 rpm for 3 minutes. Incubations were performed in duplicates. Supernatants were analyzed using the HPLC system coupled with tandem mass spectrometer. The elimination constant (k_{el}), half-life ($T_{1/2}$) and

intrinsic clearance (Cl_{int}) were determined in plot of ln(AUC) versus time, using linear regression analysis:

k_{el} = - slope
$T_{1/2}$ = 0.693/k_{el}
CL_{int} = (0.693/ $T_{1/2}$) x (µl incubation/mg microsomes)

4.4.4. Analysis of plasma protein binding

The binding of compounds **4k-n** as well as the reference compound (Verapamil) to human plasma proteins was evaluated using HPLC-MS/MS. The task was performed by spiking test compounds at concentration of 1 µM into mice plasma (Lampire Biological Labs, US, catalog number 7304309) and dialyzing against buffer until equilibrium is achieved. Concentrations of the compounds in both plasma and buffer were determined to calculate the percentage of plasma protein bound compounds.

The assay was performed in the 96-well equilibrium dialysis apparatus (HTDialysis, LLC). Each individual well unit consisted of 2 chambers separated by a vertically aligned dialysis membrane of predetermined pore size (MWCO 12-14 kDa). 120 µl of plasma spiked with the compound (1 µM, final solvent concentration 1%) was added to one chamber and the same aliquot of PBS buffer, pH 7.4 was added to the other chamber. After that, HTD96b dialyzer was covered with adhesive sealing film and incubated at 37°C on an orbital shaker at 100 rpm for 5 hours. An aliquot of the content of each chamber was taken and mixed with the same volume aliquot of the blank opposite matrix. In order to define non-specific loss of the compound during this assay, standard solution was created by mixing an aliquot of spiked plasma, which was incubated at 37°C without dialysis, with blank buffer. Sample of 1 µM series was diluted with 100% acetonitrile 10-fold with subsequent plasma proteins precipitation by centrifuging at 6000 rpm for 5 minutes. Incubations were performed in quadriplicates. Supernatants were analyzed using HPLC system coupled with tandem mass spectrometer. The unbound compound fraction was calculated as the peak ratio of the analyte in the buffer compartment divided by the same parameter in the corresponding plasma compartment. The following equation was used to determine the extent of plasma protein binding:

$$protein\_binding = \left(1 - \frac{peak\_area\_in\_dialysate\_buffer}{peak\_area\_in\_dialysate\_plasma}\right) \cdot 100\%$$

$$Recovery = \left(\frac{peak\_area\_in\_dialysate\_buffer + peak\_area\_in\_dialysate\_plasma}{peak\_area\_in\_s\tan dart\_solution}\right) \cdot 100\%$$

4.4.5. Caco-2 permeability determination

In each experiment, reference compounds Atenolol (Sigma-Aldrich, A7655), Propranolol (Sigma-Aldrich, P0884), Testosterone (Sigma-Aldrich, T1500) were tested along with the test compounds

in order to assess the assay suitability. The integrity of the cell monolayer was verified by measuring the transepithelial electrical resistance (TEER) for every well using the Millicell-ERS system Ohm meter.

The concentrations of compound **4k-n** in the A-B permeability assay were determined using HPLC-MS method. The LC system comprised a Shimadzu liquid chromatograph equipped with isocratic pumps (Shimadzu LC-10ADvp), an autosampler (Shimadzu SIL-HTc), a switching valve (FCV-14AH) and a degasser (Shimadzu DGU-14A). Mass spectrometric analysis was performed using an API 3000 (triple-quadrupole) instrument from AB Sciex (USA) with an electro-spray (ESI) interface. The data acquisition and system control was performed using Analyst 1.5.2 software from AB Sciex.

The formula for calculating P_{app} was as follows:

$$P_{app} = (VA / ((Area) \times (Time)) \times ([drug]_{acc} / [drug]_{initial,d})$$

Where VA – volume of transport buffer in acceptor well,
Area – surface area of the insert (equals to effective growth area of the insert - 0.31 sq.cm),
Time – time of the assay,
$[drug]_{acc}$ – concentration of test compound in acceptor well,
$[drug]_{initial,d}$ – initial concentration of test compound in a donor well.
P_{app} is expressed in 10^{-6} cm/sec.

Data obtained for the reference compounds:

Compound	Test concentration (μM)	Permeability (10^{-6} cm/s)			
		1st	2nd	Mean	SD
Atenolol	10	2.59	3.15	2.87	0.40
Propranolol	10	25.83	30.12	27.97	3.04
Testosterone	10	15.86	11.36	13.61	3.19

4.4.6 Mouse pharmacokinetic study

Animals. Male JAXC57BL/6J mice, supplied by the Laboratory Animal Centre (University of Eastern Finland, Kuopio, Finland), were housed in stainless steel cages and kept on a 12-h light/12-h dark cycle (lights on at 7:00 AM) at an ambient temperature of 22 $\pm$ 2 °C and humidity 55 $\pm$ 15 %. Pelleted food (Teklad 2016S, Envigo, the Netherlands) and fresh tap water were available *ad libitum*. Animals were 8-10 weeks old and weighed 20 to 27 g (n = 50). All experiments were performed in accordance with European Union guidelines (Directive 2010/63/EU and guidelines 2007/526/EC) and approved by the National Animal Experiment Board of Finland (project licence number ESAVI-2015-002090).

Drug administration and sampling. For intravenous and oral administration, **4k** was dissolved in 10 % β-cyclodextrin. Mice were placed into a restraining device and a bolus injection of **4k** (10 mg/kg) was given via a tail vein. Oral single dose of **4k** (10 mg/kg) was given by a plastic gavage. A dosing volume of 5 ml/kg was used. Mice were anesthetized by pentobarbital (0.1 ml/10 g, i.p.; Mebunat 60 mg/ml, Orion Pharma Finland) and decapitated 10, 30, 60, 120, 240 min after intravenous administration or 30, 60, 120, 240 and 360 min after oral administration (n=5 in each time point). Blood samples were taken by a cardiac puncture using heparinized syringe and plasma was separated by centrifugation for 10 min at 2 000 g at +4°C. The plasma samples were transferred into plastic tubes and stored at −70°C until analyzed.

Drug analysis. The concentrations of compound **4k** in the pharmacokinetic study were determined using quantitative HPLC-MS method. The LC system comprised an Agilent liquid chromatograph system (Agilent 1200 series rapid resolution LC system, Agilent Technologies, Waldbronn, Germany). Mass spectrometric analysis was performed using an Agilent 6410 Triple Quadrupole MS equipped with an electrospray ionization source (Agilent Technologies, Palo Alto, CA, USA). Data were acquired by Agilent MassHunter Workstation Acquisition software (version B.01.03).

Pharmacokinetic calculations. The apparent pharmacokinetic parameters, maximum plasma concentration (C_{max}), time to reach C_{max} (T_{max}), area under curve (AUC), and clearance (Cl) were calculated from group data by using a linear trapezoidal rule with linear interpolation and Phoenix WinNonlin 6.3 software (Pharsight/Cetara, Princeton, NJ, USA). No compound **4k** was detected in plasma at 360 min after oral administration and thus, 360 min time point was excluded from pharmacokinetic calculations. Oral bioavailability (F) was calculated using the following equation:

$$F = AUC_{0-\infty \text{ oral}}/AUC_{0-\infty \text{ i.v.}} \times 100 \text{ \%}.$$

Acknowledgements

Supplementary data

Supplementary data associated with this article can be found, in the online version, at http://dx.doi.org/xxx.

References and notes

1.   Briscoe, C. P.; Tadayyon, M.; Andrews, J. L.; Benson, W. G.; Chambers, J. K.; Eilert, M. M.; Ellis, C.; Elshourbagy, N. A.; Goetz, A. S.; Minnick, D. T.; Murdock, P. R.; Sauls, H. R.; Shabon, U.; Spinage, L. D.; Strum, J. C.; Szekeres, P. G.; Tan, K. B.; Way, J. M.; Ignar, D. M.; Wilson, S.; Muir, A. I. *J. Biol. Chem.* **2003**, *278*, 11303−11311.

2.   Itoh, Y.; Kawamata, Y.; Harada, M.; Kobayashi, M.; Fujii, R.; Fukusumi, S.; Ogi, K.; Hosoya, M.; Tanaka, Y.; Uejima, H.; Tanaka, H.; Maruyama, M.; Satoh, R.; Okubo, S.; Kizawa, H.; Komatsu, H.; Matsumura, F.; Noguchi, Y.; Shinohara, T.; Hinuma, S.; Fujisawa, Y.; Fujino, M. *Nature* **2003**, 422, 173-176.

3.   Watterson, K. R.; Hudson, B. D.; Ulven, T.; Milligan, G. *Front. Endocrinol.* **2014**, *5*, 137.

4.   Defossa, E.; Wagner, M. *Bioorg. Med. Chem. Lett.* **2014**, *24*, 2991-3000.

5.   https://clinicaltrials.gov, last accessed on July 21, 2016.

6.   Kaku, K.; Enya, K.; Nakaya, R.; Ohira, T.; Matsuno, R. *Diabetes Obes. Metab.* **2015**, *17*, 675-681.

7.   Mancini, A. D.; Poitout, V. *Diabetes Obes. Metab.* **2015**, *17*, 622-629.

8.   Zahanich, I.; Kondratov, I.; Naumchyk, V.; Kheylik, Y.; Platonov, M.; Zozulya, S.; Krasavin, M. *Bioorg. Med. Chem. Lett.* **2015**, *25*, 3105-3111.

9.   Krasavin, M.; Lukin, A.; Zhurilo, N.; Kovalenko, A.; Zahanich, I.; Zozulya, S. *J. Enzyme Inhib. Med. Chem.* **2016**, DOI: 10.3109/14756366.2016.1142984.

10. Krasavin, M.; Lukin, A.; Zhurilo, N.; Kovalenko, A.; Zahanich, I.; Zozulya, S.; Moore, D.; Tikhonova, I. G. *Bioorg. Med. Chem.* **2016**, *24*, 2954-2963.

11. Zheng, Y.; Tice, C. M.; Singh, S. B. *Bioorg. Med. Chem. Lett.* **2014**, *24*, 3673-3682.

12. Pastor, I. M.; Yus, M. *Curr. Org. Chem.* **2007**, *11*, 925-957.

13. Ghosh, A. K.; Shin, D.; Schiltz, G. *Heterocycles* **2002**, *58*, 659-666.

14. Lukin, A.; Bagnyukova, D.; Kalichenkova, N.; Zhurilo, N.; Krasavin, M. *Tetrahedron Lett.* **2016**, *57*, 3311-3314.

15. (a) Borzilleri, R. M.; Perez, H. L.; Wei, D. D.; Kim, K. S. PCT Int. Appl. WO 2014025759A1; *Chem. Abstr.* **2014**, *160*, 341383; (b) Amombo, G. M.; Kramer, T.; Lo Monte, Fabio; Goering, S.; Fach, M.; Smith, S.; Kolb, S.; Schubenel, R.; Baumann, K.; Schmidt, B. *Bioorg. Med. Chem. Lett.* **2012**, *22*, 7634-7640.

16. Briscoe, C. P.; Peat, A. J.; McKeown, S. C.; Corbett, D. F.; Goetz, A. S.; Littleton, T. R.; McCoy, D. C.; Kenakin, T. P.; Andrews, J. L.; Ammala, C.; Fornwald, J. A.; Ignar, D. M.; Jenkinson, S. *Br. J. Pharmacol.* **2006**, *148*, 619-628.

17. Ichimura, A.; Hirasawa, A.; Hara, T.; Tsujimoto, G. *Prostaglandins Other Lipid Mediat.* **2009**, *89*, 82-88.

18. Negoro, N.; Sasaki, S.; Mikami, S.; Ito, M.; Suzuki, M.; Tsujihata, Y.; Ito, R.; Harada, A.; Takeuchi, K.; Suzuki, N.; Miyazaki, J.; Santou, T.; Odani, T.; Kanzaki, N.; Funami, M.; Tanaka, T.; Kogame, A.; Matsunaga, S.; Yasuma, T.; Momose, Y. *ACS Med. Chem. Lett.* **2010**, *1*, 290-294.

19. Brown, J. A.; Goldsworthy, S. M.; Barnes, A. A.; Ellert, M. M.; Tcheang, L.; Daniels, D.; Muir, A. I.; Wogglesworth, M. J.; Kinghorn, I.; Fraser, N. J.; Pike, N. B.; Sturn, J. C.; Steplewski, K. M; Murdoch, P. R.; Holder, J. C.; Marshall, F. H.; Szekeres, P. G.; Wilson, S.; Ignar, D. M.; Foord, M. S.; Wise, A.; Dowell, S. J. *J. Biol. Chem.* **2003**, *278*, 11312-11319.

20. Hirasawa, A.; Tsumaya, K.; Awaji, T.; Katsuma, S.; Adachi, T.; Yamada, M.; Sugimoto, Y.; Miyazaki, S.; Tsujimoto, G. *Nat. Med.* **2005**, *11*, 90-94.

21. Ballesteros, J.; Weinstein, H. *Biophys. J.* **1995**, *68*, A446.

22. Smith, D. A.; Di, L.; Kerns, E. H. *Nat. Rev. Drug Discov.* **2010**, *9*, 929-939.

23. Srivastava, A.; Yano, J.; Hirozane, Y.; Kefala, G.; Gruswitz, F.; Snell, G.; Lane, W.; Ivetac, A.; Aertgeerts, K.; Nguyen, J.; Jennings, A.; Okada, K. *Nature* **2014**, *513*, 124-129.

24. Schrödinger, Maestro version 10.5, LLC, New York, NY, 2016.

25. Sastry, G. M.; Adzhigirey, M.; Day, T.; Annabhimoju, R.; Sherman, W. *J. Comput. Aid. Mol. Des.* **2013**, *27*, 221–234.

26. Tikhonova, I. G.; Poerio, E. *BMC Structural Biology* **2015**, *15*, 16.

27. Schrödinger, Macromodel version 11.1, LLC, New York, NY, 2016.

28. Lomize, M. A.; Pogozheva, I. D.; Joo, H.; Mosberg, H. I.; Lomize, A. L. OPM database and PPM web server: resources for positioning of proteins in membranes. *Nucleic Acids Res.* **2012**, *40*, D370-376.

29. Schrödinger, Ligprep version 3.7, LLC, New York, NY, 2016.

30. Friesner, R. A.; Banks, J. L.; Murphy, R. B.; Halgren, T. A.; Klicic, J. J.; Mainz, D. T.; Repasky, M. P.; Knoll, E. H.; Shelley, M.; Perry, J. K.; Shaw, D. E.; Francis, P.; Shenkin, P. S. *J. Med. Chem.* **2004**, *47*, 1739-1749.

31. Humphrey, W.; Dalke, A.; Schulten, K. *J. Mol. Graph.* **1996**, *14*, 33-38.

32. Hill, J. R. In Current Protocols in Pharmacology 7.8.1-7.8.11, Wiley Interscience, 2003.